

Rethinking Meta-Learning from a Learning Lens

Jingyao Wang^{1,2}, Wenwen Qiang^{1,2}, Jiangmeng Li^{1,2}, Lingyu Si^{1,2}, Changwen Zheng^{1,2}

¹University of Chinese Academy of Sciences

²National Key Laboratory of Space Integrated Information System, Institute of Software Chinese Academy of Sciences

Abstract

Meta-learning has emerged as a powerful approach for leveraging knowledge from previous tasks to solve new tasks. The mainstream methods focus on training a well-generalized model initialization, which is then adapted to different tasks with limited data and updates. However, it pushes the model overfitting on the training tasks. Previous methods mainly attributed this to the lack of data and used augmentations to address this issue, but they were limited by sufficient training and effective augmentation strategies. In this work, we focus on the more fundamental “learning to learn” strategy of meta-learning to explore what causes errors and how to eliminate these errors without changing the environment. Specifically, we first rethink the algorithmic procedure of meta-learning from a “learning” lens. Through theoretical and empirical analyses, we find that (i) this paradigm faces the risk of both overfitting and underfitting and (ii) the model adapted to different tasks promote each other where the effect is stronger if the tasks are more similar. Based on this insight, we propose using task relations to calibrate the optimization process of meta-learning and propose a plug-and-play method called Task Relation Learner (TRLearner) to achieve this goal. Specifically, it first obtains task relation matrices from the extracted task-specific meta-data. Then, it uses the obtained matrices with relation-aware consistency regularization to guide optimization. Extensive theoretical and empirical analyses demonstrate the effectiveness of TRLearner.

Introduction

Meta-learning, also known as learning to learn, usually learns a prior model from multiple tasks so that the learned model is able to quickly adapt to unseen tasks. Recently, meta-learning has demonstrated tremendous success in few-shot learning with various applications, such as affective computing (Wang et al. 2024c), image classification (Chen et al. 2021), and robotics (Schrum et al. 2022).

The mainstream methods mainly include two types (Hospedales et al. 2021): (i) optimization-based methods that learn a general model initialization; and (ii) metric-based methods that learn a transferable metric space. Unfortunately, metric-based methods are only applicable to classification problems (Sun 2023; Li et al. 2018a). In contrast, optimization-based methods are sufficiently flexible

and general to be independent of problems (Yao et al. 2021). Thus, this is also the focus of our work.

One influential approach is model-agnostic meta-learning (MAML) (Finn, Abbeel, and Levine 2017), which has inspired many subsequent extensions (Song et al. 2022; Raghu et al. 2019a,b; Li et al. 2017). However, MAML uses over-parameterized models for rapid adaptation but trained on limited data that are much smaller than the parameter dimension, making the model prone to overfitting (Chen et al. 2019; Wang et al. 2023b). Previous methods (Chen, Lu, and Chen 2022; Chua, Lei, and Lee 2021; Fallah, Mokhtari, and Ozdaglar 2021) mainly attributed this issue to the lack of data or the lack of information contained in the data. They proposed to use data augmentation or constraining data covariance matrix to eliminate overfitting. Despite the improved performance, they rely on sufficient training and effective augmentation strategies, which highly increase the training cost and perform poorly in practice applications like military and medical. In contrast, we focus on the more fundamental learning strategy to explore: (i) what causes meta-learning errors, and (ii) how to eliminate these errors without changing the environment (e.g., data) and model structure.

We begin by rethinking the “learning to learn” strategy of meta-learning. Generally, the goal of MAML can be explained as learning a model \mathcal{F}_θ that given any task τ_i , it can output a task-specific model f_θ^i that performs well, i.e., $\mathcal{F}_\theta(\tau_i) = f_\theta^i$. Existing literature (Finn, Abbeel, and Levine 2017; Nichol and Schulman 2018) defines meta-learning as bi-level optimization: (i) the first-level is for “learn”, which obtains task-specific model f_θ^i for task τ_i by optimizing \mathcal{F}_θ once on that task (Eq.1); (ii) the second-level is for “learning”, which optimizes \mathcal{F}_θ by evaluating the performance of obtained task-specific models on multiple tasks. In contrast, we propose to understand meta-learning from a single-level perspective, i.e., the “learning” of \mathcal{F}_θ . Specifically, \mathcal{F}_θ is trained to be well-generalized on multiple training tasks and then adapted to each task with one step of gradient descent. We propose that the formulation of \mathcal{F}_θ consists of parameters θ and gradient optimization. Among them, parameters θ can be further divided into the learnable parameters of a multi-layer network and a nonlinear function. The former participates in the gradient optimization of θ to obtain a well-generalized model, while the latter only propagates the gradient without updating. Through this paradigm, we

find that existing meta-learning faces both overfitting and underfitting issues from two aspects: (i) from learnable parameters: for few-shot tasks, despite the nonlinear function of \mathcal{F}_θ only contains few parameters, the large number of learnable parameters are also trained on limited data, leading to overfitting; and (ii) from gradient optimization: for complex tasks, e.g., augmented tasks (Rajendran, Irpan, and Jang 2020), \mathcal{F}_θ only performing gradient descent once for adaptation, leading to underfitting. Therefore, meta-learning still faces the issues of underfitting and overfitting. The empirical results shown in Figure 1 also prove this.

To eliminate these errors without changing the data, we first conduct theoretical analyses from the model performance of \mathcal{F}_θ . Firstly, overfitting comes from that the model mainly remembers all task-specific information rather than learning from effective information in the task (Kuhn et al. 2013). Through theoretical derivation, we find that the optimization of \mathcal{F}_θ on similar tasks is mutually promoting, and the effect is stronger if the tasks are more similar (Theorem 1). Therefore, we propose to introduce task relations to make model learn more effective information without changing data. Next, underfitting mainly comes from the limited of information within the task or insufficient learning (Wang et al. 2024b; Chen, Lu, and Chen 2022). Similarly, by extracting additional task relations, the model \mathcal{F}_θ will acquire more information to avoid underfitting. Thus, we propose to use task relations to calibrate the optimization of \mathcal{F}_θ .

Based on this insight, we propose a plug-and-play method, called Task Relation Learner (TRLearner). It aim to leverage task relations to calibrate the meta-learning optimization process. Specifically, in each training batch, TR-Learner first computes a task relation matrix based on the extracted task-specific meta-data. These meta-data contain the discriminative information of each task, and are extracted via an adaptive sampler. Then, TRLearner uses the obtained matrix to introduce relation-aware consistency regularization to the second-level optimization, constraining the update of the meta-learning model. Extensive theoretical and empirical analyses demonstrate the effectiveness of TR-Learner. In summary, the main contributions are as follows:

- We rethink the “learning to learn” strategy of meta-learning and theoretically find that (i) this paradigm faces the risk of overfitting or underfitting, and (ii) the model adapted to different tasks promote each other, which is stronger if the tasks are more similar.
- We propose TRLearner, a plug-and-play method that uses task relations and relation-aware consistency regularization to calibrate the meta-learning process.
- We theoretically prove that TRLearner improves the generalization of meta-learning with a tighter bound.
- We empirically demonstrate the effectiveness of TR-Learner on meta-learning with extensive experiments.

Related Work

Meta-Learning seeks to acquire general knowledge from various training tasks and then apply this knowledge to new tasks. Typical approaches fall into two categories: optimization-based (Finn, Abbeel, and Levine 2017; Nichol

and Schulman 2018; Wang et al. 2023a) and metric-based methods (Snell, Swersky, and Zemel 2017; Sung et al. 2018). They both acquire general knowledge from multiple training tasks with limited data to solve new tasks. In comparison, the application of metric-based methods is limited to classification problems and is not feasible in scenarios such as regression; while optimization-based methods learn generalized model initialization from meta-training tasks, are independent of the problem, and adaptable to various scenarios. However, optimization-based meta-learning still faces the challenge of performance degradation, which significantly impairs the generalization to novel tasks. Several strategies have been proposed to address this issue, such as reducing inter-task disparities (Jamal and Qi 2019), adding adaptive noise (Lee et al. 2020), and task augmentation (Yao et al. 2021). Despite these methods helping mitigate performance degradation, they still face two limitations: (i) rely on the assumption that more tasks have more general knowledge for learning, and the augmentation may be difficult to achieve in some sensitive scenarios, e.g., medicine and military; and (ii) rely on sufficient training to learn enhanced sample knowledge, which highly. They all eliminate errors by changing data but ignore the impact of the “learning to learn” strategy of meta-learning. Different from the previous works, in this study, we rethink the learning paradigm to explore what causes errors and how to eliminate these errors with theoretical and empirical supports.

Preliminaries

Meta-learning aims to bootstrap the model’s learning capabilities from a pool of tasks to accelerate the learning process when faced with a new task. These tasks are assumed to originate from a predetermined distribution $p(\mathcal{T})$, represented as $\tau \sim p(\mathcal{T})$. Given the distribution $p(\mathcal{T})$, both the meta-training dataset \mathcal{D}_{tr} and the meta-test dataset \mathcal{D}_{te} are drawn from $p(\mathcal{T})$ without any overlap in classes. During the meta-training phase, each batch includes N_{tr} tasks, represented as $\{\tau_i\}_{i=1}^{N_{tr}} \in \mathcal{D}_{tr}$. Each task τ_i comprises a support set $\mathcal{D}_i^s = \{(x_{i,j}^s, y_{i,j}^s)\}_{j=1}^{N_i^s}$ and a query set $\mathcal{D}_i^q = \{(x_{i,j}^q, y_{i,j}^q)\}_{j=1}^{N_i^q}$. Here, $(x_{i,j}, y_{i,j})$ denotes the sample and its corresponding label, and N_i indicates the number of samples, $N_i^s + N_i^q = N_i^{tr}$. The meta-learning model $\mathcal{F}_\theta = h \circ g$ employs the feature extractor g and the head h to learn these tasks. The optimal \mathcal{F}_θ^* can serve as a general initial prior, aiding task-specific models in adapting quickly to new tasks.

The model \mathcal{F}_θ performs learning via bi-level optimization. In the first level, it fine-tunes desired model f_θ^i for task τ_i by training it on the support set \mathcal{D}_i^s using the meta-learning model \mathcal{F}_θ . The objective can be represented as:

$$\begin{aligned} f_\theta^i &\leftarrow \mathcal{F}_\theta - \alpha \nabla_{\mathcal{F}_\theta} \mathcal{L}(\mathcal{D}_i^s, \mathcal{F}_\theta), \\ s.t. \quad \mathcal{L}(\mathcal{D}_i^s, \mathcal{F}_\theta) &= \frac{1}{N_i^s} \sum_{j=1}^{N_i^s} y_{i,j}^s \log \mathcal{F}_\theta(x_{i,j}^s), \end{aligned} \quad (1)$$

where α denotes the learning rate. At the second level, the meta-learning model \mathcal{F}_θ is learned using the query sets \mathcal{D}^q of all training tasks and the fine-tuned task-specific models

for each task. The objective can be represented as:

$$\begin{aligned} \mathcal{F}_\theta &\leftarrow \mathcal{F}_\theta - \beta \nabla_{\mathcal{F}_\theta} \frac{1}{N_{tr}} \sum_{i=1}^{N_{tr}} \mathcal{L}(\mathcal{D}_i^q, f_\theta^i), \\ \text{s.t. } \mathcal{L}(\mathcal{D}_i^q, f_\theta^i) &= \frac{1}{N_i^q} \sum_{j=1}^{N_i^q} y_{i,j}^q \log f_\theta^i(x_{i,j}^q), \end{aligned} \quad (2)$$

where β is the learning rate. Note that f_θ^i is derived by taking the derivative of \mathcal{F}_θ , making f_θ^i a function of \mathcal{F}_θ . Consequently, updating \mathcal{F}_θ as described in Eq. 2 can be interpreted as computing the second derivative of \mathcal{F}_θ .

Rethinking Learning to Learn

In this section, we rethink the ‘‘learning to learn’’ strategy of meta-learning from the ‘‘learning’’ lens. Then, we conduct empirical and theoretical analyses for further discussion. More details are provided in Appendix.

Reformulation of Meta-Learning Meta-learning aims to obtain a model \mathcal{F}_θ that given any task τ_i with data \mathcal{D}_i^{tr} , it can output the task-specific model f_θ^i that has the minimum $\mathbb{E}_{(x,y) \in \mathcal{D}_i} [\ell(f_\theta^i(x), y)]$. i.e., $\mathcal{F}_\theta(\tau_i) = f_\theta^i$. To learn a well-generalized \mathcal{F}_θ , we propose the formulation of \mathcal{F}_θ consists of parameters θ and gradient optimization. Specifically, θ can be divided into the learnable parameters, i.e., be updated to get well-generalized model initialization via gradient optimization, and a nonlinear function, e.g., recognize task and only propagate the gradient without updating. The previously defined bi-level meta-learning optimization can be regarded as updating these two parts of parameters separately, i.e., the learning of \mathcal{F}_θ . Through this definition, we find that meta-learning faces both overfitting and underfitting from the two components of \mathcal{F}_θ : **(i) From the learnable parameters:** in few-shot tasks, the training data is much smaller than the dimension of θ , especially the learnable part, leading overfitting. **(ii) From the gradient optimization:** in complex tasks, e.g., tasks sampled from Imagenet compared to Omniglot, \mathcal{F}_θ uses just one gradient descent step to adapt to each task during training, leading underfitting.

Empirical Evidence To verify the above views, we conduct a toy experiment. Specifically, we sample 20 sets of tasks from miniImagenet (Vinyals et al. 2016) based on (Wang et al. 2024b). We select the top four tasks with the highest scores as $\mathcal{D}_1 - \mathcal{D}_4$, and the bottom four tasks as $\mathcal{D}_5 - \mathcal{D}_8$. The higher the sampling scores, the more complex the task, and the more information the model learns. Then, we perform four-times data augmentation on $\mathcal{D}_1 - \mathcal{D}_4$. Next, we evaluate the adaptation of the MAML model on these 8 sets of tasks, i.e., perform one gradient descent and record the accuracy. The results are shown in Figure 1. We observe that: (i) models trained on \mathcal{D}_8 and \mathcal{D}_7 have an inflection point, indicating overfitting; (ii) the effect of the models on \mathcal{D}_1 is lower than the result after convergence, indicating underfitting. Thus, existing meta-learning methods do face the limitations of overfitting and underfitting, which come from the learning paradigm and will lead to errors.

Theoretical Analyses Next, we conduct theoretical analyses from model performance to explore how to eliminate these errors without changing the data. Following (Hawkins

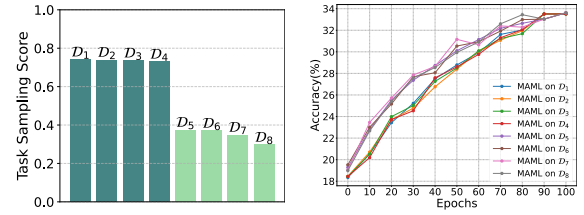


Figure 1: Motivating evidence with **Left:** average task sampling scores and **Right:** results of models trained on different task sets. More details are shown in Appendix F.

2004; Kuhn et al. 2013), for overfitting, the model should focus on effective high-level features rather than remembering all task-specific features; for underfitting, the model should focus on how to extract more information from limited data, such as increasing task complexity. Considering that existing methods perform learning via the samples within each task, i.e., intra-task relations (Yao, Zhang, and Finn 2021; Kasuga et al. 2022), we propose to introduce additional inter-task relations to improve model performance without changing the data. To verify this claim, we consider the scenario of two binary classification tasks for simple explanations. Given tasks τ_i and τ_j with data variables, X_i and X_j , and label variables, Y_i and Y_j from $\{\pm 1\}$, for one batch, we assume each task consists of task-shared factors and task-specific factors following (Pearl 2009). Then, we have:

Theorem 1 *Regardless of whether the correlation between Y_i and Y_j is equal to 0.5, the optimal classifier for τ_i has non-zero weights for task-specific factors of τ_j with importance ζ , where $\zeta \propto \text{sim}(X_i, X_j)$ and sim means similarity.*

Through Theorem 1, the learned classifier for a specific task leverages the factors from other tasks to facilitate the learning of the target task. Thus, in each training batch, the models learned from different tasks promote each other, which is stronger if the tasks are more similar. The proof is provided in Appendix B. This inspires us to use task relations to improve the effect of the meta-learning model \mathcal{F}_θ , eliminating overfitting and underfitting without changing the data.

Method

Based on this insight, in this section, we introduce Task Relation Learner (TRLearner), which uses task relation to calibrate the optimization process of meta-learning. Specifically, we first extract task relations from the sampled task-specific meta-data, obtaining the task relation matrix (**First Subsection**). The elements in this matrix reflect the similarity between tasks. Then, we use the task relation matrix to constrain the meta-learning process (**Second Subsection**), i.e., introducing relation-aware consistency regularization to the second-level optimization. The framework is shown in Figure 2, and the pseudo-code is shown in Appendix A.

Extracting Task Relations

We first discuss how to obtain the task relation matrix $\mathcal{M} = \{m_{ij}\}_{i=1, j \neq i}^{N_{tr}}$ between different tasks. Here, each element

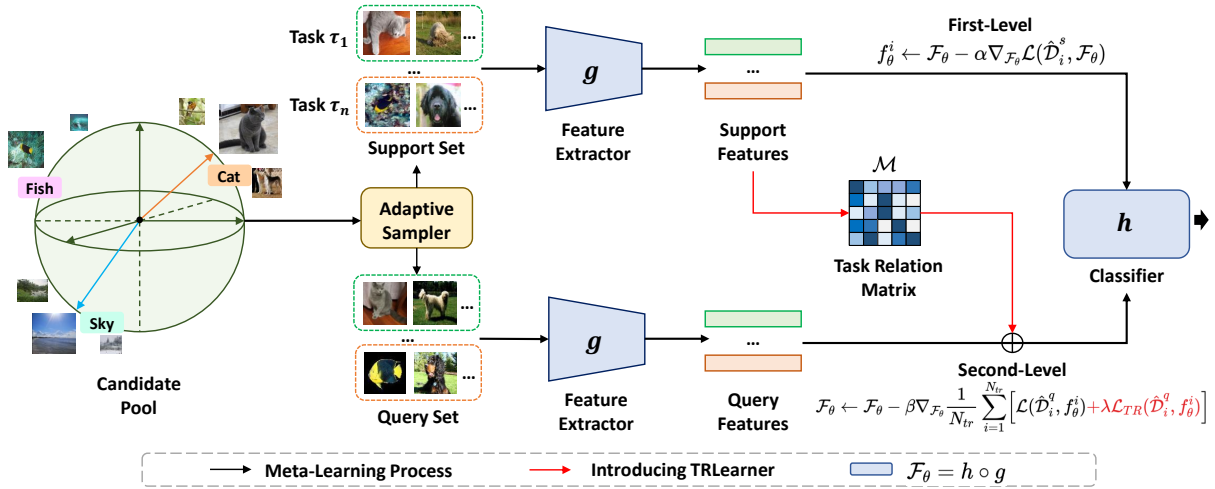


Figure 2: An illustration of the meta-learning process with TRLearner. TRLearner uses the calculated task relation matrix \mathcal{M} and the relation-aware consistency regularization term \mathcal{L}_{TR} to calibrate optimization. The black line represents the original meta-learning optimization process, while the red line represents the calibration of meta-learning by TRLearner.

m_{ij} quantifies the strength of the relationship between tasks τ_i and τ_j , N_{tr} denotes the number of tasks. Note that directly obtaining task relations from fixed task data that are randomly sampled may cause errors (Wang et al. 2024b). Taking the drug target binding affinity prediction task as an example, protein-protein interactions can be used to simulate the relationship between different proteins, but it is difficult to define in advance that two proteins must interact. Therefore, we need to constrain the acquisition of task-specific meta-data and adopt an adaptive method to quickly learn \mathcal{M} .

Specifically, we first adopt an adaptive sampler based on (Wang et al. 2024b) to obtain meta-data for each task. The data need to reflect the discriminative information and the differences between tasks, e.g., geographic proximity for cities. Correspondingly, the adaptive sampler considers four important indicators to perform task sampling, i.e., intra-class compaction, inter-class separability, feature space enrichment, and causal invariance, which constrain the discriminativeness and effectiveness of the sampled data. The higher the scores of these four indicators, the greater the sampling probability. Next, taking task τ_i and task τ_j as examples, we denote their meta-data for support set as $\hat{\mathcal{D}}_i^s$ and $\hat{\mathcal{D}}_j^s$. We first input them into the meta-learning model \mathcal{F}_θ and learn the corresponding task representations $g(\hat{\mathcal{D}}_i^s)$ and $g(\hat{\mathcal{D}}_j^s)$ with the feature extractor g . Next, we use a multi-headed similarity layer to calculate the similarity between task τ_i and task τ_j with the learnable weight matrix \mathcal{W} :

$$m_{i,j} = \frac{1}{K} \sum_{k=1}^K \cos(\omega_k \odot g(\hat{\mathcal{D}}_i^s), \omega_k \odot g(\hat{\mathcal{D}}_j^s)), \quad (3)$$

where K denotes the number of heads, \odot denotes the Hadamard product, and $\{\omega_k\}_{k=1}^K$ denotes the learnable vectors of \mathcal{W} which shares the same dimensions as the task representation, e.g., $g(\hat{\mathcal{D}}_i^s)$. It serves the purpose of accentuating variations across the different dimensions within the

vector space. Note that the initial weights of the matrix are all 1, i.e., $\omega_k = 1$, where Eq.3 is fine-tuned from $\omega_k = 1$. To this end, we obtain the task relation matrix \mathcal{M} .

Calibrating Meta-Learning

In this subsection, we present how TRLearner calibrates the optimization of meta-learning models.

Specifically, we adopt a multi-head neural network architecture consisting of a task-shared feature extractor g and N_{tr} heads $h = (h_1, \dots, h_{N_{tr}})$, where N_{tr} represents the number of tasks in a training batch for meta-learning. We define the obtained meta-data for each task τ_i as $\hat{\mathcal{D}}_i$, which are divided as a support set $\hat{\mathcal{D}}_i^s$ and a query set $\hat{\mathcal{D}}_i^q$. In the first-level of meta-learning, the meta-learning model \mathcal{F}_θ fine-tunes desired model f_θ^i for each task τ_i through g and h_i by training on $\hat{\mathcal{D}}_i^s$ using f_θ . Obtaining all B task-specific models, TRLearner calculates the task relation matrix via Eq.3. The objective of the first-level meta-learning after introducing TRLearner is almost the same as Eq.1, expressed as:

$$\begin{aligned} f_\theta^i &\leftarrow \mathcal{F}_\theta - \alpha \nabla_{\mathcal{F}_\theta} \mathcal{L}(\hat{\mathcal{D}}_i^s, \mathcal{F}_\theta), \\ s.t. \quad \mathcal{L}(\hat{\mathcal{D}}_i^s, \mathcal{F}_\theta) &= \frac{1}{N_i^s} \sum_{j=1}^{N_i^s} y_{i,j}^s \log \mathcal{F}_\theta(x_{i,j}^s), \end{aligned} \quad (4)$$

where α denotes the learning rate.

Then, in the second-level optimization, the meta-learning model \mathcal{F}_θ is learned using the query sets $\hat{\mathcal{D}}^q$ of all training tasks, the fine-tuned task-specific models for each task, and the task relation matrix obtained in the first-level. Compared to Eq.2, the improved second-level optimization additionally considers the task relations calculated by TRLearner to calibrate the optimization process. To introduce this, a simple approach is to directly use the task relation score, i.e., $m_{i,j}$, to weight different task-specific models. The higher the similarity between tasks, the higher the weight assigned to the task for second-level optimization. However, this weighting method is often affected by the distribution of tasks in the

training batch and may lead to cumulative errors. Therefore, TRLearner exploits the assumption that similar tasks tend to have similar prediction functions and introduces a relation-aware consistency regularization term to replace the rough weighting. Given sample $(x_{i,j}, y_{i,j})$ in task τ_i , the regularization term combines the task relations to weight the predictions generated by all other task-specific models except the model f_θ^i for τ_i . Take task τ_i as an example, the regularization term $\mathcal{L}_{TR}(\hat{\mathcal{D}}_i^q, f_\theta^i)$ can be expressed as:

$$\mathcal{L}_{TR}(\hat{\mathcal{D}}_i^q, f_\theta^i) = \frac{1}{N_i^q} \sum_{j=1}^{N_i^q} \ell\left(\frac{\sum_{p=1, p \neq i}^{N_{tr}} m_{ip} f_\theta^p(x_{ij})}{\sum_{q=1, q \neq i}^{N_{tr}} m_{iq}}, y_{i,j}\right), \quad (5)$$

where m_{ip} is defined as the strength of the relation between task τ_i and τ_p , $\ell(\cdot)$ is the loss that promotes the alignment of the ground truth with the weighted average prediction obtained from all other task-specific models, leveraging task relations to apportion their respective influences. \mathcal{L}_{TR} encourages the meta-learning model to reinforce the interconnections among task-specific models, placing greater trust in predictions from similar tasks while diminishing reliance on those from disparate tasks. Then, the objective of the second-level optimization can be expressed as:

$$\begin{aligned} \mathcal{F}_\theta &\leftarrow \mathcal{F}_\theta - \beta \nabla_{\mathcal{F}_\theta} \frac{1}{N_{tr}} \sum_{i=1}^{N_{tr}} \left[\mathcal{L}(\hat{\mathcal{D}}_i^q, f_\theta^i) + \lambda \mathcal{L}_{TR}(\hat{\mathcal{D}}_i^q, f_\theta^i) \right], \\ \text{s.t. } \mathcal{L}(\hat{\mathcal{D}}_i^q, f_\theta^i) &= \frac{1}{N_i^q} \sum_{j=1}^{N_i^q} y_{i,j}^q \log f_\theta^i(x_{i,j}^q), \end{aligned} \quad (6)$$

where β is the learning rate and λ is the importance weight of \mathcal{L}_{TR} . By doing so, meta-learning can obtain better \mathcal{F}_θ to adapt to various downstream tasks without changing its objective or training data, i.e., $\mathcal{F}_\theta(\tau_i) = f_\theta^i$.

Theoretical Analysis

In this section, we conduct theoretical analyses to evaluate whether task relations can improve the performance of meta-learning. Specifically, we first provide an upper bound on the excess risk, showing that by considering the task relations, we can bridge the gap between training and testing tasks (**Theorem 2**). Next, we show that by leveraging the accurate task relations, we can achieve better generalization than previous methods that treat all training tasks equally (**Theorem 3**). The proofs are provided in Appendix B.

We first provide the assumptions to facilitate analysis.

Assumption 1 For each task τ_i , the representation Z_i of task τ_i is derived from the task-specific meta-data $\hat{\mathcal{D}}_i$ via the feature extractor g of meta-learning model $f_\theta = h \circ g$, where $h = (h_1, \dots, h_{N_{tr}})$. Then, we assume:

- Z_i is assumed to be uniformly distributed on $[0, 1]^k$.
- There exists a universal constant C such that for all $i, j \in N_{tr}$, we have $\|h_i - h_j\|_\infty \leq C \cdot \|Z_i - Z_j\|$.
- The relation between task τ_i and τ_j , i.e., $m_{i,j}$, is determined by the distance between the representations Z_i and Z_j with a bandwidth σ , i.e., $m_{i,j} = \{\|Z_i - Z_j\| < \sigma\}$.
- The head \hat{h}_i from the well-learned model \mathcal{F}_θ^* such that $\mathbb{E} \left[(\hat{h}_i(g(x)) - h_i(g(x)))^2 \right] = \mathcal{O}\left(\frac{\mathcal{R}(\mathcal{H})}{N_{tr}^i}\right)$ where $\mathcal{R}(\mathcal{H})$ is the Rademacher complexity of the head class \mathcal{H} .

Next, we provide the maximum limit of excess risk.

Theorem 2 Assume that for every task, the training data \mathcal{D}_i^{tr} contains N_i^{tr} that is approximately greater than or equal to the minimum number of samples found across all tasks, i.e., N_{sh} . If the loss function $\ell(\cdot)$ is Lipschitz continuous concerning its first parameter, then for the test task τ^{te} , the excess risk adheres to the following condition:

$$\sum_{(x,y) \in \mathcal{D}^{te}} [\ell(\mathcal{F}_\theta^*(x), y) - \ell(\mathcal{F}_\theta(x), y)] \leq \sigma + \sqrt{\frac{\mathcal{R}(\mathcal{H})}{N_{sh} N_{tr} \sigma^k}}, \quad (7)$$

where N_{tr} denotes the number of tasks, while the other symbols, e.g., σ , k , etc., are the same as in Assumption 1.

It suggests that incorporating task relations can bridge the gap between training and test tasks, resulting in a decrease in the excess risk as the number of training tasks increases.

Next, we demonstrate that obtaining an accurate task relation matrix \mathcal{M} can enhance the OOD generalization of meta-learning. Specifically, our method aims to obtain the task relation matrix \mathcal{M} that reflects the real similarity between tasks based on TRLearner and introduces it into meta-learning optimization. In contrast, we denote the matrix corresponding to the previous meta-learning method as $\check{\mathcal{M}}$, where all elements are set to 1. Given \mathcal{M} and $\check{\mathcal{M}}$, we get:

Theorem 3 Consider the function class \mathcal{H} that satisfies Assumption 1 and the same conditions as Theorem 2, define the excess risk with task relation matrix \mathcal{M} by $r(\mathcal{F}_\theta^*, \mathcal{M}) = \sum_{(x,y) \in \mathcal{D}^{te}} [\ell(\mathcal{F}_\theta^*(x), y; \mathcal{M}) - \ell(\mathcal{F}_\theta(x), y; \mathcal{M})]$, we have $\inf_{\mathcal{F}_\theta^*} \sup_{h \in \mathcal{H}} r(\mathcal{F}_\theta^*, \mathcal{M}) - \inf_{\mathcal{F}_\theta^*} \sup_{h \in \mathcal{H}} r(\mathcal{F}_\theta^*, \check{\mathcal{M}}) < 0$.

This theorem shows that introducing \mathcal{M} achieves better generalization of model \mathcal{F}_θ compared to $\check{\mathcal{M}}$, i.e., having smaller excess risk. Thus, our TRLearner effectively enhances the generalization of meta-learning with theoretical support.

Experiments

To evaluate the effectiveness of TRLearner, we conduct experiments on four meta-learning problems, i.e., (i) regression (**First Subsection**), (ii) image classification (**Second Subsection**), (iii) drug activity prediction (**Third Subsection**), and (iv) pose prediction (**Fourth Subsection**). We apply TRLearner to four optimization-based meta-learning algorithms, including MAML (Finn, Abbeel, and Levine 2017), MetaSGD (Li et al. 2017), ANIL (Raghu et al. 2019a), and T-NET (Lee and Choi 2018). For comparison, we consider the following regularizers which handle meta-learning generalization, i.e., Meta-Aug (Rajendran, Irpan, and Jang 2020), MetaMix (Yao et al. 2021), Dropout-Bins (Jiang et al. 2022) and MetaCRL (Wang et al. 2023a), and the SOTA methods which are newly proposed for generalization, i.e., Meta-Trans (Bengio et al. 2019), MR-MAML (Yin et al. 2020), iMOL (Wu et al. 2023), OOD-MAML (Jeong and Kim 2020), and RotoGBML (Zhang et al. 2023). We also conduct ablation studies to evaluate how TRLearner works well (**Fifth Subsection**). All results are averaged from five runs, performed using NVIDIA V100 GPUs. More details and analyses are provided in Appendices C-F.

Model	(Sin,5-shot)	(Sin,10-shot)	(Har,5-shot)	(Har,10-shot)
MR-MAML	0.581 ± 0.110	0.104 ± 0.029	0.590 ± 0.125	0.247 ± 0.089
Meta-Trans	0.577 ± 0.123	0.097 ± 0.024	0.576 ± 0.116	0.231 ± 0.074
iMOL	0.572 ± 0.107	0.083 ± 0.018	0.563 ± 0.108	0.228 ± 0.062
OOD-MAML	0.553 ± 0.112	0.076 ± 0.021	0.552 ± 0.103	0.224 ± 0.058
RotoGBML	0.546 ± 0.104	0.061 ± 0.012	0.539 ± 0.101	0.216 ± 0.043
MAML	0.593 ± 0.120	0.166 ± 0.061	0.622 ± 0.132	0.256 ± 0.099
MAML+Meta-Aug	0.531 ± 0.118	0.103 ± 0.031	0.596 ± 0.127	0.247 ± 0.094
MAML+MetaMix	0.476 ± 0.109	0.085 ± 0.024	0.576 ± 0.114	0.236 ± 0.097
MAML+Dropout-Bins	0.452 ± 0.081	0.062 ± 0.017	0.561 ± 0.109	0.235 ± 0.056
MAML+MetaCRL	0.440 ± 0.079	0.054 ± 0.018	0.548 ± 0.103	0.211 ± 0.071
MAML+TRLearner	0.400 ± 0.064	0.052 ± 0.016	0.539 ± 0.101	0.204 ± 0.037
ANIL	0.541 ± 0.118	0.103 ± 0.032	0.573 ± 0.124	0.205 ± 0.072
ANIL+Meta-Aug	0.536 ± 0.115	0.097 ± 0.026	0.561 ± 0.119	0.197 ± 0.064
ANIL+MetaMix	0.514 ± 0.106	0.083 ± 0.022	0.554 ± 0.113	0.184 ± 0.053
ANIL+Dropout-Bins	0.487 ± 0.110	0.088 ± 0.025	0.541 ± 0.104	0.179 ± 0.035
ANIL+MetaCRL	0.468 ± 0.094	0.081 ± 0.019	0.533 ± 0.083	0.153 ± 0.031
ANIL+TRLearner	0.471 ± 0.081	0.075 ± 0.023	0.517 ± 0.074	0.134 ± 0.028
MetaSGD	0.577 ± 0.126	0.152 ± 0.044	0.612 ± 0.138	0.248 ± 0.076
MetaSGD+Meta-Aug	0.524 ± 0.122	0.138 ± 0.027	0.608 ± 0.126	0.231 ± 0.069
MetaSGD+MetaMix	0.468 ± 0.118	0.072 ± 0.023	0.595 ± 0.117	0.226 ± 0.062
MetaSGD+Dropout-Bins	0.435 ± 0.089	0.040 ± 0.011	0.578 ± 0.109	0.213 ± 0.057
MetaSGD+MetaCRL	0.408 ± 0.071	0.038 ± 0.010	0.551 ± 0.104	0.195 ± 0.042
MetaSGD+TRLearner	0.391 ± 0.057	0.024 ± 0.008	0.532 ± 0.101	0.176 ± 0.027
T-NET	0.564 ± 0.128	0.111 ± 0.042	0.597 ± 0.135	0.214 ± 0.078
T-NET+Meta-Aug	0.521 ± 0.124	0.105 ± 0.031	0.584 ± 0.122	0.207 ± 0.063
T-NET+MetaMix	0.498 ± 0.113	0.094 ± 0.025	0.576 ± 0.119	0.183 ± 0.054
T-NET+Dropout-Bins	0.470 ± 0.091	0.077 ± 0.028	0.559 ± 0.113	0.174 ± 0.035
T-NET+MetaCRL	0.462 ± 0.078	0.071 ± 0.019	0.554 ± 0.112	0.158 ± 0.024
T-NET+TRLearner	0.443 ± 0.058	0.066 ± 0.012	0.543 ± 0.102	0.144 ± 0.013

Table 1: Performance (MSE) comparison on the Sinusoid and Harmonic regression. The best results are highlighted in **bold**, and TRLearner’s results are highlighted in **green**.

Performance on Regression

Experimental Setup We conduct experiments on (i) Sinusoid dataset (Jiang et al. 2022) with 480 tasks which are generated from $A \sin w \cdot x + b + \epsilon$, where $A \in [0.1, 5.0]$, $w \in [0.5, 2.0]$, and $b \in [0, 2\pi]$. Gaussian observation noise with a mean (μ) of 0 and a standard deviation (ϵ) of 0.3 is added to each sampled data point; and (ii) Harmonic dataset (Wang et al. 2024b) with 480 tasks sampled from a sum of two sine waves with different phases, amplitudes, and a frequency ratio of 2, i.e., $f(x) = a_1 \sin(\omega x + b_1) + a_2 \sin(2\omega x + b_2)$, where $y \sim \mathcal{N}(f(x), \sigma_y^2)$ where $\mathcal{U}(5, 7)$, (b_1, b_2) from $\mathcal{U}(0, 2\pi)^2$, and (a_1, a_2) from $\mathcal{N}(0, 1)^2$. We use the Mean Squared Error (MSE) as the evaluation metric.

Results As shown in Table 1, we can observe that (i) TR-Learner achieves similar and more stable improvements to the SOTA baselines, with average MSE reduced by 0.028 and 0.021 respectively; (ii) TRLearner also shows significant improvements in all meta-learning base models, with MSE reduced by more than 0.1; (iii) after the introduction of TRLearner, some meta-learning baselines achieve better results than methods that focus on generalization. Thus, TR-Learner enhances the generalization of meta-learning.

Performance on Image Classification

Experimental Setup We select two image classification environments, i.e., standard few-shot learning (SFSL) and cross-domain few-shot learning (CFSL), with four benchmark datasets, i.e., miniImagenet (Vinyals et al. 2016), Omniglot (Lake, Salakhutdinov, and Tenenbaum 2019), CUB (Welinder et al. 2010), and Places (Zhou et al. 2017). Among them, the setting of CFSL strengthens the distribution difference of data during model training and testing, which can

Model	Omniglot	miniImagenet	→CUB	→Places
MR-MAML	89.28 ± 0.59	35.01 ± 1.60	35.76 ± 1.27	31.23 ± 0.48
Meta-Trans	87.39 ± 0.51	35.19 ± 1.58	36.21 ± 1.36	31.97 ± 0.52
iMOL	92.89 ± 0.44	36.27 ± 1.54	37.14 ± 1.17	32.44 ± 0.65
OOD-MAML	93.01 ± 0.50	37.43 ± 1.47	39.62 ± 1.34	35.52 ± 0.69
RotoGBML	92.77 ± 0.69	39.32 ± 1.62	41.27 ± 1.24	35.32 ± 0.58
MAML	87.15 ± 0.61	33.16 ± 1.70	33.62 ± 1.18	29.84 ± 0.56
MAML+Meta-Aug	89.77 ± 0.62	34.76 ± 1.52	34.58 ± 1.24	30.57 ± 0.63
MAML+MetaMix	91.97 ± 0.51	38.97 ± 1.81	36.29 ± 1.37	31.76 ± 0.49
MAML+Dropout-Bins	92.89 ± 0.46	39.66 ± 1.74	37.41 ± 1.12	33.69 ± 0.78
MAML+MetaCRL	93.00 ± 0.42	41.55 ± 1.76	38.16 ± 1.27	35.41 ± 0.53
MAML+TRLearner	94.23 ± 0.56	42.86 ± 1.83	40.54 ± 1.26	36.12 ± 0.64
ANIL	89.17 ± 0.56	34.96 ± 1.71	35.74 ± 1.16	31.64 ± 0.57
ANIL+Meta-Aug	90.46 ± 0.47	35.44 ± 1.73	36.32 ± 1.28	32.58 ± 0.64
ANIL+MetaMix	92.88 ± 0.51	37.82 ± 1.75	36.89 ± 1.34	33.72 ± 0.61
ANIL+Dropout-Bins	92.82 ± 0.49	38.09 ± 1.76	38.24 ± 1.17	33.94 ± 0.66
ANIL+MetaCRL	92.91 ± 0.52	38.55 ± 1.81	39.68 ± 1.32	34.47 ± 0.52
ANIL+TRLearner	93.24 ± 0.48	38.73 ± 1.84	41.96 ± 1.24	35.68 ± 0.61
MetaSGD	87.81 ± 0.61	33.97 ± 0.92	33.65 ± 1.13	29.83 ± 0.66
MetaSGD+Meta-Aug	88.56 ± 0.57	35.76 ± 0.91	34.73 ± 1.32	31.49 ± 0.54
MetaSGD+MetaMix	93.44 ± 0.45	40.28 ± 0.96	35.26 ± 1.21	32.76 ± 0.59
MetaSGD+Dropout-Bins	93.93 ± 0.40	40.31 ± 0.96	37.49 ± 1.37	33.21 ± 0.67
MetaSGD+MetaCRL	94.12 ± 0.43	41.22 ± 0.93	38.61 ± 1.25	35.83 ± 0.63
MetaSGD+TRLearner	94.57 ± 0.49	41.64 ± 0.94	39.58 ± 1.13	36.42 ± 0.54
T-NET	87.66 ± 0.59	33.69 ± 1.72	34.82 ± 1.17	28.77 ± 0.48
T-NET+Meta-Aug	91.29 ± 0.53	35.24 ± 1.74	35.42 ± 1.28	30.54 ± 0.57
T-NET+MetaMix	93.16 ± 0.48	39.18 ± 1.73	37.22 ± 1.37	31.28 ± 0.61
T-NET+Dropout-Bins	93.54 ± 0.49	39.06 ± 1.72	37.49 ± 1.14	32.37 ± 0.55
T-NET+MetaCRL	93.81 ± 0.52	40.08 ± 1.74	38.47 ± 1.36	33.69 ± 0.48
T-NET+TRLearner	94.33 ± 0.54	40.31 ± 1.75	40.64 ± 1.29	34.76 ± 0.62

Table 2: Performance (accuracy ± 95% confidence interval) of image classification on SFSL, i.e., (20-way 1-shot) Omniglot and (5-way 1-shot) miniImagenet, and CFSL settings, i.e., miniImagenet → CUB and miniImagenet → Places.

better reflect its OOD generalization performance. The evaluation metric employed here is the average accuracy.

Results Table 2 shows the comparison results under SFSL and CFSL settings. We can observe that: (i) Under the SFSL setting, the introduction of TRLearner achieves stable performance improvement and surpasses other comparison baselines, including regularizers and methods that focus on meta-learning generalization; (ii) Under the CFSL setting, TRLearner always surpasses the SOTA baseline, indicating that it can achieve better generalization improvement without introducing task-specific or label space augmentations required by the baseline. Combined with the comparative experiment of the trade-off performance (accuracy vs. training time) in Appendix F, TRLearner achieves the best generalization improvement under the condition of lower computational cost. This further proves the superiority of TRLearner.

Performance on Drug Activity Prediction

Experimental Setup We also assess TRLearner for drug activity prediction using the pQSAR dataset (Martin et al. 2019), which forecasts compound activity on specific target proteins and includes 4,276 tasks. Following (Martin et al. 2019; Yao et al. 2021), we divide the tasks into four groups but conduct the “Group 5” that contains tasks randomly drawn from the other four groups for average evaluation. The evaluation metric is the squared Pearson correlation coefficient (R^2), indicating the correlation between predictions and actual values for each task. We report the mean and median R^2 values, as well as the count of R^2 values exceeding 0.3, which is a reliable indicator in pharmacology.

Model	Group 1			Group 2			Group 3			Group 4			Group 5 (ave)		
	Mean	Med.	> 0.3	Mean	Med.	> 0.3	Mean	Med.	> 0.3	Mean	Med.	> 0.3	Mean	Med.	> 0.3
MAML	0.371	0.315	52	0.321	0.254	43	0.318	0.239	44	0.348	0.281	47	0.341	0.260	45
MAML+Dropout-Bins	0.410	0.376	60	0.355	0.257	48	0.320	0.275	46	0.370	0.337	56	0.380	0.314	52
MAML+MetaCRL	0.413	0.378	61	0.360	0.261	50	0.334	0.282	51	0.375	0.341	59	0.371	0.316	56
MAML+TRLearner	0.418	0.380	62	0.366	0.263	52	0.342	0.285	52	0.379	0.339	59	0.378	0.319	56
ANIL	0.355	0.296	50	0.318	0.297	49	0.304	0.247	46	0.338	0.301	50	0.330	0.284	48
ANIL+MetaMix	0.347	0.292	49	0.302	0.258	45	0.301	0.282	47	0.348	0.303	51	0.327	0.284	48
ANIL+Dropout-Bins	0.394	0.321	53	0.338	0.271	48	0.312	0.284	46	0.368	0.297	50	0.350	0.271	49
ANIL+TRLearner	0.402	0.341	57	0.347	0.276	49	0.320	0.296	48	0.374	0.306	53	0.364	0.304	51

Table 3: Performance comparison on drug activity prediction. “Mean”, “Med.”, and “> 0.3” are the mean, the median value of R^2 , and the number of analyzes for $R^2 > 0.3$. The best results are highlighted in **bold**.

Model	10-shot	15-shot
MAML	3.113 ± 0.241	2.496 ± 0.182
MAML + MetaMix	2.429 ± 0.198	1.987 ± 0.151
MAML + Dropout-Bins	2.396 ± 0.209	1.961 ± 0.134
MAML + MetaCRL	2.355 ± 0.200	1.931 ± 0.134
MAML + TRLearner	2.334 ± 0.216	1.875 ± 0.132
MetaSGD	2.811 ± 0.239	2.017 ± 0.182
MetaSGD + MetaMix	2.388 ± 0.204	1.952 ± 0.134
MetaSGD + Dropout-Bins	2.369 ± 0.217	1.927 ± 0.120
MetaSGD + MetaCRL	2.362 ± 0.196	1.920 ± 0.191
MetaSGD + TRLearner	2.357 ± 0.188	1.893 ± 0.176
T-NET	2.841 ± 0.177	2.712 ± 0.225
T-NET + MetaMix	2.562 ± 0.280	2.410 ± 0.192
T-NET + Dropout-Bins	2.487 ± 0.212	2.402 ± 0.178
T-NET + MetaCRL	2.481 ± 0.274	2.400 ± 0.171
T-NET + TRLearner	2.476 ± 0.248	2.398 ± 0.167

Table 4: Performance (MSE ± 95% confidence interval) comparison on pose prediction.

Results As shown in Table 3, TRLearner achieves comparable performance to the SOTA baselines. Consider that drug activity prediction is a more complex task, and the difference between the mean and median of the model’s R^2 score is larger (Martin et al. 2019). TRLearner not only narrows the gap between the model’s R^2 Mean and R^2 Median scores but also achieves an improvement in the reliability index $R^2 > 0.3$. This observation further demonstrates TRLearner’s superior performance in more complex scenarios.

Performance on Pose Prediction

Experimental Setup We use the Pascal 3D dataset (Xiang, Mottaghi, and Savarese 2014) on pose prediction with the evaluation metric being MSE. We randomly select 50 objects for training and an additional 15 objects for testing.

Results As shown in Table 4, TRLearner achieves results close to or even exceeding the SOTA baseline without additional data. Particularly, studies (Yao et al. 2021) have shown that augmentations in pose prediction can expand the data to make the model acquire more knowledge, thus achieving better results. The fact that TRLearner can achieve similar improvements further proves its effectiveness.

Ablation Study

Effect of \mathcal{L}_{TR} We evaluate the performance of MAML before and after introducing \mathcal{L}_{TR} on miniImagenet, where

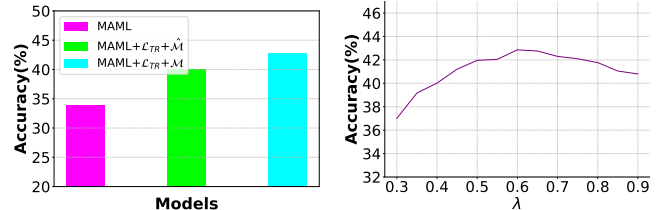


Figure 3: Effect of \mathcal{L}_{TR} on Accuracy (%) for miniImagenet.

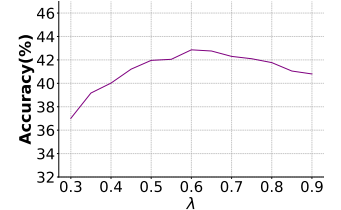


Figure 4: Parameter sensitivity on miniImagenet.

\mathcal{L}_{TR} is the core of TRLearner. We also evaluate the adaptive learning method of the task relation matrix \mathcal{M} by replacing it with a fixed calculation, i.e., directly calculating the similarity between the sampled meta-data ($\hat{\mathcal{M}}$). As shown in Figure 3, (i) the model achieves significant performance improvement with negligible computational overhead after introducing \mathcal{L}_{TR} ; (ii) the adaptively learned \mathcal{M} is more accurate than the fixed calculation. This proves the effectiveness of TRLearner and the forward-looking design.

Parameter Sensitivity We determine the hyperparameters λ of the regularization term \mathcal{L}_{TR} by evaluating the performance across multiple meta-validation tasks. We test the impact of different values of λ on the performance of MAML+TRLearner with the range $[0.3, 0.8]$. The results in Figure 4 show that (i) $\lambda = 0.6$ is the best (also our setting), and (ii) TRLearner has minimal variation in accuracy, indicating that hyperparameter tuning is easy in practice.

Conclusion

In this paper, we rethink the “learning to learn” strategy of meta-learning and find that (i) the learning paradigm faces the limitations of overfitting and underfitting; and (ii) the adapted models for different tasks promote each other where the promotion is related to task relations, with theoretical and empirical supports. Then, we propose TRLearner, a novel plug-and-play method that uses task relation to calibrate the meta-learning process, thus eliminating errors without changing the environment and model structure. It uses relation-aware consistency regularization to incorporate the extracted task relation matrix into meta-learning’s bi-level optimization process. Extensive theoretical and empirical analyses demonstrate the effectiveness of TRLearner.

References

- Barrett, D. G.; and Dherin, B. 2020. Implicit gradient regularization. *arXiv preprint arXiv:2009.11162*.
- Bengio, Y.; Deleu, T.; Rahaman, N.; Ke, R.; Lachapelle, S.; Bilaniuk, O.; Goyal, A.; and Pal, C. 2019. A meta-transfer objective for learning to disentangle causal mechanisms. *arXiv preprint arXiv:1901.10912*.
- Bohdal, O.; Yang, Y.; and Hospedales, T. 2021. Meta-calibration: Learning of model calibration using differentiable expected calibration error. *arXiv preprint arXiv:2106.09613*.
- Boutillier, C.; Hsu, C.-w.; Kveton, B.; Mladenov, M.; Szepesvari, C.; and Zaheer, M. 2020. Differentiable meta-learning of bandit policies. *Advances in Neural Information Processing Systems*, 33: 2122–2134.
- Chen, L.; Lu, S.; and Chen, T. 2022. Understanding benign overfitting in gradient-based meta learning. *Advances in neural information processing systems*, 35: 19887–19899.
- Chen, W.-Y.; Liu, Y.-C.; Kira, Z.; Wang, Y.-C. F.; and Huang, J.-B. 2019. A closer look at few-shot classification. *arXiv preprint arXiv:1904.04232*.
- Chen, Y.; Guan, C.; Wei, Z.; Wang, X.; and Zhu, W. 2021. Metadelta: A meta-learning system for few-shot image classification. In *AAAI Workshop on Meta-Learning and MetaDL Challenge*, 17–28. PMLR.
- Choe, S.; Mehta, S. V.; Ahn, H.; Neiswanger, W.; Xie, P.; Strubell, E.; and Xing, E. 2024. Making scalable meta learning practical. *Advances in neural information processing systems*, 36.
- Choe, S. K.; Neiswanger, W.; Xie, P.; and Xing, E. 2022. Betty: An automatic differentiation library for multilevel optimization. *arXiv preprint arXiv:2207.02849*.
- Chua, K.; Lei, Q.; and Lee, J. D. 2021. How fine-tuning allows for effective meta-learning. *Advances in Neural Information Processing Systems*, 34: 8871–8884.
- Fallah, A.; Mokhtari, A.; and Ozdaglar, A. 2021. Generalization of model-agnostic meta-learning algorithms: Recurring and unseen tasks. *Advances in Neural Information Processing Systems*, 34: 5469–5480.
- Finn, C.; Abbeel, P.; and Levine, S. 2017. Model-agnostic meta-learning for fast adaptation of deep networks. In *International conference on machine learning*, 1126–1135. PMLR.
- Flennerhag, S.; Rusu, A. A.; Pascanu, R.; Visin, F.; Yin, H.; and Hadsell, R. 2019. Meta-learning with warped gradient descent. *arXiv preprint arXiv:1909.00025*.
- Gaulton, A.; Bellis, L. J.; Bento, A. P.; Chambers, J.; Davies, M.; Hersey, A.; Light, Y.; McGlinchey, S.; Michalovich, D.; Al-Lazikani, B.; et al. 2012. ChEMBL: a large-scale bioactivity database for drug discovery. *Nucleic acids research*, 40(D1): D1100–D1107.
- Hawkins, D. M. 2004. The problem of overfitting. *Journal of chemical information and computer sciences*, 44(1): 1–12.
- Hospedales, T.; Antoniou, A.; Micaelli, P.; and Storkey, A. 2021. Meta-learning in neural networks: A survey. *IEEE transactions on pattern analysis and machine intelligence*, 44(9): 5149–5169.
- Jamal, M. A.; and Qi, G.-J. 2019. Task agnostic meta-learning for few-shot learning. In *Proceedings of the IEEE/CVF Conference on Computer Vision and Pattern Recognition*, 11719–11727.
- Jeong, T.; and Kim, H. 2020. Ood-maml: Meta-learning for few-shot out-of-distribution detection and classification. *Advances in Neural Information Processing Systems*, 33: 3907–3916.
- Jiang, Y.; Chen, Z.; Kuang, K.; Yuan, L.; Ye, X.; Wang, Z.; Wu, F.; and Wei, Y. 2022. The Role of Deconfounding in Meta-learning. In *International Conference on Machine Learning*, 10161–10176. PMLR.
- Kasuga, S.; Heming, E.; Lowrey, C.; and Scott, S. H. 2022. High intra-task and low inter-task correlations of motor skills in humans creates an individualized behavioural pattern. *Scientific Reports*, 12(1): 20156.
- Khadka, R.; Jha, D.; Hicks, S.; Thambawita, V.; Riegler, M. A.; Ali, S.; and Halvorsen, P. 2022. Meta-learning with implicit gradients in a few-shot setting for medical image segmentation. *Computers in Biology and Medicine*, 143: 105227.
- Kuhn, M.; Johnson, K.; Kuhn, M.; and Johnson, K. 2013. Over-fitting and model tuning. *Applied predictive modeling*, 61–92.
- Lacoste, A.; Oreshkin, B.; Chung, W.; Boquet, T.; Ros-tamzadeh, N.; and Krueger, D. 2018. Uncertainty in multitask transfer learning. *arXiv preprint arXiv:1806.07528*.
- Lake, B. M.; Salakhutdinov, R.; and Tenenbaum, J. B. 2019. The Omniglot challenge: a 3-year progress report. *Current Opinion in Behavioral Sciences*, 29: 97–104.
- Lee, H. B.; Nam, T.; Yang, E.; and Hwang, S. J. 2020. Meta dropout: Learning to perturb latent features for generalization.
- Lee, J.; Tack, J.; Lee, N.; and Shin, J. 2021. Meta-learning sparse implicit neural representations. *Advances in Neural Information Processing Systems*, 34: 11769–11780.
- Lee, Y.; and Choi, S. 2018. Gradient-based meta-learning with learned layerwise metric and subspace. In *International Conference on Machine Learning*, 2927–2936. PMLR.
- Li, D.; Yang, Y.; Song, Y.-Z.; and Hospedales, T. 2018a. Learning to generalize: Meta-learning for domain generalization. In *Proceedings of the AAAI conference on artificial intelligence*, volume 32.
- Li, D.; Yang, Y.; Song, Y.-Z.; and Hospedales, T. 2018b. Learning to generalize: Meta-learning for domain generalization. In *Proceedings of the AAAI conference on artificial intelligence*, volume 32.
- Li, Z.; Zhou, F.; Chen, F.; and Li, H. 2017. Meta-sgd: Learning to learn quickly for few-shot learning. *arXiv preprint arXiv:1707.09835*.
- Lin, M.; Li, W.; Li, D.; Chen, Y.; Li, G.; and Lu, S. 2023. Multi-domain generalized graph meta learning. In *Proceedings of the AAAI Conference on Artificial Intelligence*, volume 37, 4479–4487.

- Liu, R.; Bai, F.; Du, Y.; and Yang, Y. 2022. Meta-reward-net: Implicitly differentiable reward learning for preference-based reinforcement learning. *Advances in Neural Information Processing Systems*, 35: 22270–22284.
- Martin, E. J.; Polyakov, V. R.; Zhu, X.-W.; Tian, L.; Mukherjee, P.; and Liu, X. 2019. All-assay-Max2 pQSAR: activity predictions as accurate as four-concentration IC50s for 8558 Novartis assays. *Journal of chemical information and modeling*, 59(10): 4450–4459.
- Nichol, A.; Achiam, J.; and Schulman, J. 2018. On first-order meta-learning algorithms. *arXiv preprint arXiv:1803.02999*.
- Nichol, A.; and Schulman, J. 2018. Reptile: a scalable meta-learning algorithm. *arXiv preprint arXiv:1803.02999*, 2(3): 4.
- Pearl, J. 2009. *Causality*. Cambridge university press.
- Raghu, A.; Raghu, M.; Bengio, S.; and Vinyals, O. 2019a. Rapid learning or feature reuse? towards understanding the effectiveness of maml. *arXiv preprint arXiv:1909.09157*.
- Raghu, A.; Raghu, M.; Bengio, S.; and Vinyals, O. 2019b. Rapid learning or feature reuse? towards understanding the effectiveness of maml. *arXiv preprint arXiv:1909.09157*.
- Rajendran, J.; Irpan, A.; and Jang, E. 2020. Meta-learning requires meta-augmentation. *NeurIPS*.
- Rajeswaran, A.; Finn, C.; Kakade, S. M.; and Levine, S. 2019. Meta-learning with implicit gradients. *Advances in neural information processing systems*, 32.
- Schrump, M. L.; Hedlund-Botti, E.; Moorman, N.; and Gombolay, M. C. 2022. Mind meld: Personalized meta-learning for robot-centric imitation learning. In *2022 17th ACM/IEEE International Conference on Human-Robot Interaction (HRI)*, 157–165. IEEE.
- Snell, J.; Swersky, K.; and Zemel, R. 2017. Prototypical networks for few-shot learning. *Advances in neural information processing systems*, 30.
- Song, X.; Zheng, S.; Cao, W.; Yu, J.; and Bian, J. 2022. Efficient and effective multi-task grouping via meta learning on task combinations. *Advances in Neural Information Processing Systems*, 35: 37647–37659.
- Sun, Y. 2023. Meta learning in decentralized neural networks: towards more general AI. In *Proceedings of the AAAI Conference on Artificial Intelligence*, volume 37, 16137–16138.
- Sung, F.; Yang, Y.; Zhang, L.; Xiang, T.; Torr, P. H.; and Hospedales, T. M. 2018. Learning to compare: Relation network for few-shot learning. In *Proceedings of the IEEE conference on computer vision and pattern recognition*, 1199–1208.
- Triantafillou, E.; Zhu, T.; Dumoulin, V.; Lamblin, P.; Evci, U.; Xu, K.; Goroshin, R.; Gelada, C.; Swersky, K.; Manzagol, P.-A.; et al. 2019. Meta-dataset: A dataset of datasets for learning to learn from few examples. *arXiv preprint arXiv:1903.03096*.
- Vinyals, O.; Blundell, C.; Lillicrap, T.; Wierstra, D.; et al. 2016. Matching networks for one shot learning. *Advances in neural information processing systems*, 29.
- Wang, J.; Qiang, W.; Li, J.; Si, L.; Zheng, C.; and Su, B. 2024a. On the Causal Sufficiency and Necessity of Multi-Modal Representation Learning. *arXiv preprint arXiv:2407.14058*.
- Wang, J.; Qiang, W.; Ren, Y.; Song, Z.; Zhang, J.; and Zheng, C. 2023a. Hacking Task Confounder in Meta-Learning. *arXiv preprint arXiv:2312.05771*.
- Wang, J.; Qiang, W.; Su, X.; Zheng, C.; Sun, F.; and Xiong, H. 2024b. Towards Task Sampler Learning for Meta-Learning. *International Journal of Computer Vision*, 1–31.
- Wang, J.; Qiang, W.; and Zheng, C. 2024. Explicitly Modeling Generality into Self-Supervised Learning. *arXiv preprint arXiv:2405.01053*.
- Wang, J.; Tian, Y.; Yang, Y.; Chen, X.; Zheng, C.; and Qiang, W. 2024c. Meta-Auxiliary Learning for Micro-Expression Recognition. *arXiv preprint arXiv:2404.12024*.
- Wang, J.; and Yu, N. 2022. So-perm: Pose estimation and robust measurement for small objects. In *2022 International Joint Conference on Neural Networks (IJCNN)*, 1–7. IEEE.
- Wang, J.; Zhang, C.; Ding, Y.; and Yang, Y. 2023b. Awesome-META+: Meta-Learning Research and Learning Platform. *arXiv preprint arXiv:2304.12921*.
- Welinder, P.; Branson, S.; Mita, T.; Wah, C.; Schroff, F.; Belongie, S.; and Perona, P. 2010. Caltech-UCSD birds 200.
- Wu, X.; Lu, J.; Fang, Z.; and Zhang, G. 2023. Meta OOD Learning For Continuously Adaptive OOD Detection. In *Proceedings of the IEEE/CVF International Conference on Computer Vision*, 19353–19364.
- Xiang, Y.; Mottaghi, R.; and Savarese, S. 2014. Beyond pascal: A benchmark for 3d object detection in the wild. In *IEEE winter conference on applications of computer vision*, 75–82. IEEE.
- Yao, H.; Huang, L.-K.; Zhang, L.; Wei, Y.; Tian, L.; Zou, J.; Huang, J.; et al. 2021. Improving generalization in meta-learning via task augmentation. In *International conference on machine learning*, 11887–11897. PMLR.
- Yao, H.; Zhang, L.; and Finn, C. 2021. Meta-learning with fewer tasks through task interpolation. *arXiv preprint arXiv:2106.02695*.
- Yin, M.; Tucker, G.; Zhou, M.; Levine, S.; and Finn, C. 2020. Meta-Learning without Memorization. *ICLR*.
- Zhang, B.; Luo, C.; Yu, D.; Li, X.; Lin, H.; Ye, Y.; and Zhang, B. 2024. Metadiff: Meta-learning with conditional diffusion for few-shot learning. In *Proceedings of the AAAI Conference on Artificial Intelligence*, volume 38, 16687–16695.
- Zhang, M.; Zhuang, Z.; Wang, Z.; Wang, D.; and Li, W. 2023. Rotogbml: Towards out-of-distribution generalization for gradient-based meta-learning. *arXiv preprint arXiv:2303.06679*.
- Zhou, B.; Lapedriza, A.; Khosla, A.; Oliva, A.; and Torralba, A. 2017. Places: A 10 million image database for scene recognition. *IEEE transactions on pattern analysis and machine intelligence*, 40(6): 1452–1464.

Reproducibility Checklist

This paper:

- Includes a conceptual outline and/or pseudocode description of AI methods introduced (yes)
- Clearly delineates statements that are opinions, hypothesis, and speculation from objective facts and results (yes)
- Provides well marked pedagogical references for less-familiale readers to gain background necessary to replicate the paper (yes)
- Does this paper make theoretical contributions? (yes)

Does this paper make theoretical contributions? (yes)

If yes, please complete the list below.

- All assumptions and restrictions are stated clearly and formally. (yes)
- All novel claims are stated formally (e.g., in theorem statements). (yes)
- Proofs of all novel claims are included. (yes)
- Proof sketches or intuitions are given for complex and/or novel results. (yes)
- Appropriate citations to theoretical tools used are given. (yes)
- All theoretical claims are demonstrated empirically to hold. (yes)
- All experimental code used to eliminate or disprove claims is included. (yes)

Does this paper rely on one or more datasets? (yes)

If yes, please complete the list below.

- A motivation is given for why the experiments are conducted on the selected datasets (yes)
- All novel datasets introduced in this paper are included in a data appendix. (yes)
- All novel datasets introduced in this paper will be made publicly available upon publication of the paper with a license that allows free usage for research purposes. (yes)
- All datasets drawn from the existing literature (potentially including authors' own previously published work) are accompanied by appropriate citations. (yes)
- All datasets drawn from the existing literature (potentially including authors' own previously published work) are publicly available. (yes)
- All datasets that are not publicly available are described in detail, with explanation why publicly available alternatives are not scientifically satisficing. (yes)

Does this paper include computational experiments? (yes)

If yes, please complete the list below.

- Any code required for pre-processing data is included in the appendix. (yes)
- All source code required for conducting and analyzing the experiments is included in a code appendix. (yes)
- All source code required for conducting and analyzing the experiments will be made publicly available upon publication of the paper with a license that allows free usage for research purposes. (yes)

- All source code implementing new methods have comments detailing the implementation, with references to the paper where each step comes from (yes)
- If an algorithm depends on randomness, then the method used for setting seeds is described in a way sufficient to allow replication of results. (yes)
- This paper specifies the computing infrastructure used for running experiments (hardware and software), including GPU/CPU models; amount of memory; operating system; names and versions of relevant software libraries and frameworks. (yes)
- This paper formally describes evaluation metrics used and explains the motivation for choosing these metrics. (yes)
- This paper states the number of algorithm runs used to compute each reported result. (yes)
- Analysis of experiments goes beyond single-dimensional summaries of performance (e.g., average; median) to include measures of variation, confidence, or other distributional information. (yes)
- The significance of any improvement or decrease in performance is judged using appropriate statistical tests (e.g., Wilcoxon signed-rank). (yes)
- This paper lists all final (hyper-)parameters used for each model/algorithm in the paper's experiments. (yes)
- This paper states the number and range of values tried per (hyper-) parameter during development of the paper, along with the criterion used for selecting the final parameter setting. (yes)

Appendix

The appendix provides supplementary information and additional details that support the primary discoveries and methodologies proposed in this paper. It is organized into several sections:

- Appendix O provides the details and further analysis about the “learning” lens of meta-learning.
- Appendix A encompasses the pseudo-code of meta-learning with TRLearner.
- Appendix B contains the proofs of the presented theorems.
- Appendix C provides details for all datasets used in the experiments.
- Appendix D provides details for the baselines used in the experiments.
- Appendix E presents the implementation and architecture of our method, aiding in the faithful reproduction of our work.
- Appendix F provides additional experiments, full results, and experimental details of the comparison experiments that were omitted in the main text due to page limitations.

Note that before we illustrate the details and analysis, we provide a brief summary of all the experiments conducted in this paper, as shown in Table 5.

O The “Learning” Lens of Meta-Learning

In this section, we further explore (i) why we rethink meta-learning from a learning lens and (ii) further analyses about the formulation of meta-learning \mathcal{F}_θ .

As mentioned in the main text, the goal of MAML can be explained as learning a model \mathcal{F}_θ that given any task τ_i , it can output a task-specific model f_θ^i that performs well, i.e., $\mathcal{F}_\theta(\tau_i) = f_\theta^i$. The previously “Learning to Learn” understanding proposes to obtain \mathcal{F}_θ through a bi-level optimization process: (i) the first-level is for “learn”, which obtains task-specific model f_θ^i for task τ_i by optimizing \mathcal{F}_θ once on that task (Eq.1); (ii) the second-level is for “learning”, which optimizes \mathcal{F}_θ by evaluating the performance of obtained task-specific models on multiple tasks.

However, there exists a gap between this theoretical understanding and the practical implementation, i.e., the update of the model \mathcal{F}_θ is mostly based on single-level optimization rather than a bi-level optimization process. Specifically, according to (Choe et al. 2022), the update methods of existing meta-learning models mainly include three types: implicit gradient (Rajeswaran et al. 2019; Barrett and Dherin 2020; Khadka et al. 2022; Flennerhag et al. 2019; Lee et al. 2021), differentiable proxies (Choe et al. 2024; Bohdal, Yang, and Hospedales 2021; Boutilier et al. 2020; Liu et al. 2022), and single-layer approximation (Nichol and Schulman 2018; Rajendran, Irpan, and Jang 2020; Nichol, Achiam, and Schulman 2018; Raghu et al. 2019a). **Appendix O.1** provides the specific forms of these three optimization methods. These methods all integrate the gradient of all tasks in the same training batch into a single optimization step to update the parameter θ . This means that the

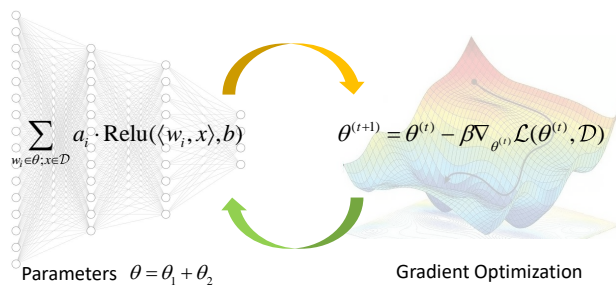


Figure 5: The reformulation of meta-learning model \mathcal{F}_θ from the learning lens, which consists of parameters θ and gradient optimization. The learning of \mathcal{F}_θ can be viewed as the interaction of these two components.

model \mathcal{F}_θ is not gradually learned and optimized through inner and outer loops, but directly adapted to multiple tasks through a single-level process. Therefore, there exists a gap between the theoretical understanding of meta-learning, i.e., the “learning to learn” strategy, and its practical implementation, i.e., the code and update of meta-learning model \mathcal{F}_θ .

To unify the theoretical concepts of meta-learning with its practical implementation, we propose to rethink meta-learning from the “Learning” lens and reformulate the meta-learning model \mathcal{F}_θ . Specifically, we propose that the formulation of \mathcal{F}_θ consists of parameters θ and gradient optimization. Figure 5 briefly illustrates the formulation of \mathcal{F}_θ . Further, the parameters θ can be further divided into the learnable parameters of a multi-layer network denoted as \mathcal{F}_{θ_1} , and a nonlinear function, denoted as \mathcal{F}_{θ_2} . Among them, \mathcal{F}_{θ_1} will be updated to get well-generalized model initialization via gradient optimization, while \mathcal{F}_{θ_2} only propagates the gradient without updating, e.g., recognize different tasks in the same batch. In the optimization process of meta-learning, each training batch contains multiple tasks, and the data of each training task is further divided into a support set and a query set. Then, \mathcal{F}_θ is first updated once based on the support set of each task, where \mathcal{F}_{θ_1} directly participates in the gradient update and \mathcal{F}_{θ_2} is used to identify different tasks and spread gradients; then the learnable parameters \mathcal{F}_{θ_1} are further updated based on the query sets of all tasks in the current batch, and the ability of \mathcal{F}_θ is improved through multiple iterations.

Through this formulation, as mentioned in Section “Rethinking Learning to Learn”, meta-learning faces both overfitting and underfitting from the two components of \mathcal{F}_θ , i.e., the learnable parameters θ and gradient optimization. Specifically, **from the learnable parameters θ** : in few-shot tasks, the training data is much smaller than the dimension of θ . Although the dimension of parameters in \mathcal{F}_{θ_2} is smaller, \mathcal{F}_{θ_1} is usually over-parameterized (Chen, Lu, and Chen 2022), e.g., Resnet-based MAML models typically have around 6 million parameters but are trained on 1-3 million meta-training data, leading to overfitting. **From the gradient optimization**: in complex tasks, e.g., tasks sampled from Imagenet compared to Omniglot, \mathcal{F}_θ uses just one

Experiments	Location	Results
Motivating experiments	Section “Rethink Learning to Learn” and Appendix F.1	Figure 1
Performance on regression problems with two benchmark datasets	Section “Performance on Regression”	Table 1
Performance on image classification with two settings, i.e., standard few-shot learning (miniImagenet and Omniglot) and cross-domain few-shot learning (miniImagenet \rightarrow CUB and Places)	Section “Performance on Image Classification” and Appendix F.2	Table 2 and Table 6
Performance on drug activity prediction (pQSAR)	Section “Performance on Drug Activity Prediction” and Appendix F.2	Table 3 and Table 7
Experiment on pose prediction (Pascal 3D)	Section “Performance on Pose Prediction” and Appendix F.2	Table 4 and Table 8
Ablation Study-Effect of \mathcal{L}_{TR}	Section “Ablation Study”	Figure 3
Ablation Study-Parameter Sensitivity	Section “Ablation Study”	Figure 4
Results Together with Other Regularizers	Appendix F.3	Table 9 and Table 10
Trade-off Performance Comparison	Appendix F.4	Figure 7
OOD Generalization Performance Comparison	Appendix F.5	Table 11
Task Relation Visualization	Appendix F.6	Figure 8

Table 5: Illustration of the experiments conducted in this work. Note that all experimental results are obtained after five rounds of experiments.

gradient descent step to adapt to each task during training, leading underfitting.

O.1 Practical Implementation of Update \mathcal{F}_θ

For a simple but clear explanation, we set the parameters of the inner loop as ϕ and the parameters of the outer loop as θ according to the concept of “learning to learn”. Then, the inner optimization problem is assumed to be $\phi^*(\theta) = \arg \min_{\phi} \mathcal{L}_{\text{inner}}(\theta, \phi)$, where θ is the outer parameter, ϕ is the parameter of inner loop, and $\mathcal{L}_{\text{inner}}$ is the loss function.

Implicit Gradient The implicit gradient method calculates the outer gradient $\nabla_{\theta} \mathcal{L}_{\text{outer}}(\theta, \phi^*(\theta))$ by solving the following equation:

$$\nabla_{\theta} \phi^*(\theta) = - [\nabla_{\phi}^2 \mathcal{L}_{\text{inner}}(\theta, \phi^*(\theta))]^{-1} \nabla_{\theta \phi}^2 \mathcal{L}_{\text{inner}}(\theta, \phi^*(\theta)), \quad (8)$$

where $\nabla_{\phi}^2 \mathcal{L}_{\text{inner}}$ is the Hessian matrix with respect to ϕ for the inner loss function. Then, the outer gradient is computed using the chain rule:

$$\nabla_{\theta} \mathcal{L}_{\text{outer}}(\theta, \phi^*(\theta)) = \nabla_{\phi} \mathcal{L}_{\text{outer}}(\theta, \phi^*(\theta)) \cdot \nabla_{\theta} \phi^*(\theta) + \nabla_{\theta} \mathcal{L}_{\text{outer}}(\theta, \phi^*(\theta)) \quad (9)$$

This allows the outer parameter θ to be updated without explicitly solving the inner loop optimization.

Differentiable Proxies In some applications, the inner optimization objective $\mathcal{L}_{\text{inner}}(\theta, \phi)$ may be difficult to compute or non-differentiable. To simplify this, a differentiable proxy function $\tilde{\mathcal{L}}_{\text{inner}}(\theta, \phi)$ can be used as a substitute:

$$\tilde{\mathcal{L}}_{\text{inner}}(\theta, \phi) \approx \mathcal{L}_{\text{inner}}(\theta, \phi).$$

Then, the proxy function is used for inner loop optimization:

$$\phi^*(\theta) = \arg \min_{\phi} \tilde{\mathcal{L}}_{\text{inner}}(\theta, \phi).$$

The outer loop optimization still targets $\mathcal{L}_{\text{outer}}(\theta, \phi^*(\theta))$.

Single-level Approximation The bi-level optimization problem is simplified. The inner loop optimization becomes:

$$\phi^i = \phi - \alpha \nabla_{\phi} \mathcal{L}_{\text{inner}}(\theta, \phi),$$

and the outer loop optimization is:

$$\min_{\theta} \sum_{i=1}^N \mathcal{L}_{\text{outer}}(\theta, \phi^i).$$

In the single-level approximation, the update from the inner loop optimization is treated as a fixed value, and ϕ is no longer iteratively optimized. The outer loop directly uses the updated ϕ^i with:

$$\min_{\theta} \sum_{i=1}^N \mathcal{L}_{\text{outer}}(\theta, \phi - \alpha \nabla_{\phi} \mathcal{L}_{\text{inner}}(\theta, \phi)).$$

In the optimization process of meta-learning model \mathcal{F}_θ , the gradient information on all tasks is integrated into a single optimization step and directly used to update the global parameter θ , which means that the model \mathcal{F}_θ is not gradually learned and optimized through internal and external loops, but directly adapted to multiple tasks through a single process. Therefore, the actual meta-learning model update method is more like a single-layer optimization process rather than true “learning to learn”, i.e., it does not strictly follow the theoretical two-layer optimization framework.

A Pseudo-code

The pseudocode of the meta-learning process with our proposed TRLearner is shown in Algorithm 1. TRLearner is a plug-and-play method that aims to improve generalization by calibrating the meta-learning optimization process based on task relations. Specifically, it first extracts task relations from the sampled task-specific meta-data, obtaining the task relation matrix. Then, it uses the task relation matrix to constrain the optimization of the meta-learning model, i.e., introducing relation-aware consistency regularization term to the second-level meta-learning, obtaining a better meta-learning model that performs well on all task adaptations.

B Proofs

In this section, we provide proofs and analyses of theorems in the main text. Before detailed proofs, we first provide the assumptions to facilitate analysis:

Assumption 1 For each task τ_i , the representation Z_i of task τ_i is derived from the task-specific meta-data $\hat{\mathcal{D}}_i$ via the feature extractor g of meta-learning model $f_\theta = h \circ g$, where $h = (h_1, \dots, h_{N_{tr}})$. Then, we assume:

- Z_i is assumed to be uniformly distributed on $[0, 1]^k$.
- There exists a universal constant C such that for all $i, j \in N_{tr}$, we have $\|h_i - h_j\|_\infty \leq C \cdot \|Z_i - Z_j\|$.
- The relation between task τ_i and τ_j , i.e., $m_{i,j}$, is determined by the distance between the representations Z_i and Z_j with a bandwidth σ , i.e., $m_{i,j} = \{\|Z_i - Z_j\| < \sigma\}$.
- The head \hat{h}_i from the well-learned model \mathcal{F}_θ^* such that $\mathbb{E} \left[(\hat{h}_i(g(x)) - h_i(g(x)))^2 \right] = \mathcal{O} \left(\frac{\mathcal{R}(\mathcal{H})}{N_i^{tr}} \right)$ where $\mathcal{R}(\mathcal{H})$ is the Rademacher complexity of the head class \mathcal{H} .

Next, we provide proofs of Theorems 1, 2, and 3 in turn.

B.1 Proof of Theorem 1

Theorem 1 Regardless of whether the correlation between Y_i and Y_j is equal to 0.5, the optimal classifier for τ_i has non-zero weights for task-specific factors of τ_j with importance ζ , where $\zeta \propto \text{sim}(X_i, X_j)$ and sim means similarity.

Proof In the analyses, we consider a simple scenario involving two binary classification tasks, denoted as τ_i and τ_j . That is, we set batchsize for training as 2. The label variables for these tasks are represented by Y_i and Y_j , respectively, while X_i and X_j denote the sample variables for the two tasks. Given that these are binary classification tasks, Y_i and Y_j belong to the set of task labels $\{\pm 1\}$. It is worth noting that any multi-classification task can be decomposed into a combination of binary tasks (one against the other classes). In this proof, we focus on binary tasks to demonstrate the task confounder more simply and directly. Meanwhile, despite the two tasks are sampled from the same distribution, in this proof, we assume that these labels are drawn from two different probabilities, and the sampling probabilities of label values are balanced, i.e., $P(Y = 1) = P(Y = -1) = 0.5$. Our conclusions also hold for imbalanced distributions.

Given the set of causal factors for the entire world, \mathbf{a}^w , the training set represents a subset of the world with causal

factors $\mathbf{a}^{tr} \subseteq \mathbf{A}^w$. Since \mathbf{a}^{tr} is unknown, we model \mathbf{a}^w using a Gaussian distribution, where the probability of a causal factor indicates its likelihood of belonging to \mathbf{a}^{tr} . For tasks τ_i and τ_j , we consider two non-overlapping sets of factors, \mathbf{a}^i and \mathbf{a}^j , representing knowledge in N_z dimensions. These factors are assumed to be drawn from Gaussian distributions, i.e., $\mathbf{a}^i \sim \mathcal{N}(Y_i \cdot \mu_i, \sigma_i^2 I)$ and $\mathbf{a}^j \sim \mathcal{N}(Y_j \cdot \mu_j, \sigma_j^2 I)$. Here, $\mu_i, \mu_j \in \mathbb{R}^{N_z}$ denote the mean vectors, while σ_i^2 and σ_j^2 denote the covariance vectors.

In this analysis, we focus on the links of different task-specific model, which reflect the performance of meta-learning model \mathcal{F}_θ and decide whether to update further. For the sake of simplicity, we define p to represent the varying correlations resulting from different task adaptations across different batches. Hence, we get:

$$\begin{aligned} P(Y_i = Y_j) &= p \\ P(Y_i \neq Y_j) &= 1 - p \end{aligned} \quad (10)$$

When p equals 0.5, it indicates that under this circumstance, the two tasks τ_i and τ_j are correlated within these environments. The objective of meta-learning adaptation is to obtain two linear models, $f_\theta^i : P(Y_i | \mathbf{a}^i, \mathbf{a}^j)$ and $f_\theta^j : P(Y_j | \mathbf{a}^i, \mathbf{a}^j)$ for τ_i and τ_j .

Next, if the task-specific model promote each other, then the optimal classifier for each task has non-zero weights for non-causal factors, i.e., the task-specific factors of another task. When training \mathcal{F}_θ using two tasks, the optimal classifier for the target task will include causal features from the other task that are non-causal factors for the target task. To demonstrate this, we assume the use of a Bayesian classifier. Using task τ_i as an example, we can derive the probability of $P(Y_i, \mathbf{A}^i, \mathbf{A}^j)$ with the optimal Bayesian classifier $P(Y_i | \mathbf{A}^i, \mathbf{A}^j)$ as follows:

$$\begin{aligned} P(Y_i, \mathbf{a}^i, \mathbf{a}^j) &= P(Y_i, \mathbf{a}^i) \cdot P(\mathbf{a}^j | Y_i, \mathbf{a}^i) \\ &= P(Y_i, \mathbf{a}^i) \cdot P(\mathbf{a}^j | Y_i) \\ &= P(Y_i, \mathbf{a}^i) \cdot \sum_{Y_j \in \{-1, 1\}} P(\mathbf{a}^j, Y_j | Y_i) \\ &= P(Y_i) P(\mathbf{a}^i | Y_i) \cdot \sum_{Y_j \in \{-1, 1\}} P(\mathbf{a}^j | Y_j) P(Y_j | Y_i) \end{aligned} \quad (11)$$

where the optimal Bayesian classifier $P(Y_i | \mathbf{A}^i, \mathbf{A}^j)$ is:

$$\begin{aligned} P(Y_i | \mathbf{a}^i, \mathbf{a}^j) &= \frac{P(Y_i, \mathbf{a}^i, \mathbf{a}^j)}{P(\mathbf{a}^i, \mathbf{a}^j)} \\ &= \frac{P(Y_i, \mathbf{a}^i, \mathbf{a}^j)}{\sum_{Y_i \in \{-1, 1\}} P(Y_i, \mathbf{a}^i, \mathbf{a}^j)} \end{aligned} \quad (12)$$

Assuming both \mathbf{a}^i and \mathbf{a}^j are drawn from Gaussian distributions, we have $P(Y_{i/j}, \mathbf{a}^i, \mathbf{a}^j) = \text{sigmoid} \left(\frac{\mu_i}{\sigma_i^2} \mathbf{a}^i + \frac{\mu_j}{\sigma_j^2} \mathbf{a}^j \right)$, where $\frac{\mu_i}{\sigma_i^2}$ and $\frac{\mu_j}{\sigma_j^2}$ are the regression vectors for the optimal Bayesian classifier. Let $\zeta^+ = \frac{\mu_i}{\sigma_i^2} \mathbf{A}^i + \frac{\mu_j}{\sigma_j^2} \mathbf{A}^j$ and

Algorithm 1: Meta-Learning with TRLearner

Input: Task distribution $p(\mathcal{T})$; Randomly initialize meta-learning model f_θ with a feature extractor g and multi-heads h ; Initialize task relation matrix $\mathcal{M} = \mathbb{I}^{N_{tr} \times N_{tr}}$

Parameter: Number of tasks for one batch N_{tr} ; Learning rates α and β for the learning of f_θ ; Loss weight λ for the relation-aware consistency regularization term

Output: Meta-learning model \mathcal{F}_θ

```

1: while not coverage do
2:   Sample tasks  $\tau \sim \{\tau_i\}_{i=1}^{N_{tr}}$  from  $p(\mathcal{T})$  via the adaptive task sampler ▷ Task Construction
3:   for all  $\tau_i$  do
4:     Obtain the support set  $\mathcal{D}_i^s = \{(x_{i,j}^s, y_{i,j}^s)\}_{j=1}^{N_i^s}$  for task  $\tau_i$ 
5:     Obtain the query set  $\mathcal{D}_i^q = \{(x_{i,j}^q, y_{i,j}^q)\}_{j=1}^{N_i^q}$  for task  $\tau_i$ 
6:     Update task relation matrix  $\mathcal{M} = \{m_{ij}\}_{i=1, j \neq i}^{N_{tr}}$  via Eq.3 ▷ Calculate Task Relation
7:     Update the task-specific model  $f_\theta^i$  using the support set  $\mathcal{D}_i^s$  of task  $\tau_i$  via Eq.4 ▷ Inner-Loop Update
8:   end for
9:   Calculate relation-aware consistency score  $\mathcal{L}_{TR}(\hat{\mathcal{D}}_i^q, f_\theta^i)$  for each task ▷ Calibrate Optimization Process
10:  Update meta-learning model  $f_\theta$  using all the query sets  $\mathcal{D}^q$  in a single batch with  $\mathcal{L}_{TR}$  via Eq.6 ▷ Outer-Loop Update
11: end while
12: return solution

```

$\zeta^- = \frac{\mu_i}{\sigma_i^2} A^i - \frac{\mu_j}{\sigma_j^2} A^j$, we first obtain:

$$\begin{aligned}
P(Y_i, a^i, a^j) &= P(Y_i, a^i) \cdot P(a^j | Y_i, a^i) \\
&= P(Y_i) P(a^i | Y_i) \cdot \sum_{Y_j \in \{-1, 1\}} P(a^j | Y_j) P(Y_j | Y_i) \\
&\propto e^{Y_i \cdot \frac{\mu_i}{\sigma_i^2} a^i} \left(p e^{Y_i \cdot \frac{\mu_j}{\sigma_j^2} a^j} + (1-p) e^{-Y_i \cdot \frac{\mu_j}{\sigma_j^2} a^j} \right) \\
&= p e^{Y_i \cdot (\frac{\mu_i}{\sigma_i^2} a^i + \frac{\mu_j}{\sigma_j^2} a^j)} + (1-p) e^{Y_i \cdot (\frac{\mu_i}{\sigma_i^2} a^i - \frac{\mu_j}{\sigma_j^2} a^j)}
\end{aligned} \tag{13}$$

Then the Bayesian classifier $P(Y_i | A^i, A^j)$ becomes:

$$P(Y_i | a^i, a^j) = \frac{1}{1 + \frac{p e^{Y_i \cdot \zeta^+} + (1-p) e^{Y_i \cdot \zeta^-}}{p e^{-Y_i \cdot \zeta^+} + (1-p) e^{-Y_i \cdot \zeta^-}}} \tag{14}$$

Next, when $p = 0.5$, i.e., the correlation between Y_i and Y_j is equal to 0.5, we get:

$$P(Y_i | a^i, a^j) = \frac{1}{1 + e^{Y_i \cdot (\zeta^+ + \zeta^-)}} = \frac{1}{1 + e^{2Y_i \cdot (\frac{\mu_j}{\sigma_j^2} a^j)}} \tag{15}$$

When $p \neq 0.5$, i.e., the correlation between Y_i and Y_j is not equal to 0.5, we get:

$$P(Y_i | a^i, a^j) = \frac{1}{1 + e^{2Y_i \cdot \zeta^+}} = \frac{1}{1 + e^{2Y_i \cdot \zeta^+}} \tag{16}$$

In both conditions, the optimal classifier for τ_i has non-zero weights for task-specific factors of τ_j with importance ζ : (i) In Eq.15, the optimal classifier for task τ_i only utilizes its factor A^i and assigns zero weights to the non-causal factor a^j which belongs to task τ_j ; (ii) In Eq.16, the optimal classifier is both for the two factors a^i and a^j . Thus, Theorem 1 is certified.

B.2 Proof of Theorem 2

Theorem 2 Assume that for every task, the training data \mathcal{D}_i^{tr} contains N_i^{tr} that is approximately greater than or

equal to the minimum number of samples found across all tasks, i.e., N_{sh} . If the loss function $\ell(\cdot)$ is Lipschitz continuous concerning its first parameter, then for the test task τ^{te} , the excess risk adheres to the following condition:

$$\sum_{(x,y) \in \mathcal{D}^{te}} [\ell(\mathcal{F}_\theta^*(x), y) - \ell(\mathcal{F}_\theta(x), y)] \leq \sigma + \sqrt{\frac{\mathcal{R}(\mathcal{H})}{N_{sh} N_{tr} \sigma^k}}, \tag{17}$$

where N_{tr} denotes the number of tasks, while the other symbols, e.g., σ , k , etc., are the same as in Assumption 1.

Proof To establish the proof of Theorem 2, we initially define a function that serves as an intermediary, which can be expressed as:

$$h_p^{in} = \frac{\sum_{i=1}^{N_{tr}} m_{ip} h_i}{\sum_{j=1}^{N_{tr}} m_{jp}} \tag{18}$$

We proceed to delineate an event, denoted as $e_{N_{sh}}$, which is characterized by the condition $\sum_{i=1}^{N_{tr}} m_{ip} > 0$. Given our presupposition that:

$$\mathbb{E}[(\mathcal{F}_\theta^*(x) - \mathcal{F}_\theta(x))^2] = \mathbb{E}[(h_i^*(g(x)) - h_i(g(x)))^2] = \mathcal{O}\left(\frac{\mathcal{R}(\mathcal{H})}{N_i^{tr}}\right), \tag{19}$$

where g denotes the feature extractor and h denotes the classifier head for meta-learning. Here, also given the relationship $N_i^{tr} \gtrsim N_{sh}$ for every task τ_i , it follows that during the occurrence of $e_{N_{sh}}$, the following inequality holds:

$$\begin{aligned}
&\mathbb{E}[(h_p^{in}(g(x)) - h_p^*(g(x)))^2] \\
&\leq \frac{\sum_{i=1}^{N_{tr}} m_{ip} \cdot \mathbb{E}[(h_i^*(g(x)) - h_i(g(x)))^2]}{(\sum_{j=1}^{N_{tr}} m_{jp})^2} \\
&\leq \frac{\max_i \mathbb{E}[(h_i^*(g(x)) - h_i(g(x)))^2]}{\sum_{j=1}^{N_{tr}} m_{jp}} \\
&= \mathcal{O}\left(\frac{\mathcal{R}(\mathcal{H})}{N_{sh} \sum_{j=1}^{N_{tr}} m_{jp}}\right).
\end{aligned} \tag{20}$$

Furthermore, given that $\|h_i - h_j\|_\infty \leq C \cdot \|Z_i - Z_j\| \leq C \cdot \sigma$ when $\|Z_i - Z_j\| \leq \sigma$, we can assert that within the scenario

$\mathbf{e}_{N_{sh}}$, the inequality $|h_k^{in} - h_k| \leq C \cdot \sigma$ is valid. Conversely, for the complementary event $\mathbf{e}_{N_{sh}}^c$, the denominator is nullified by definition, rendering $h_k^{in}(g(x)) = 0$ and thus:

$$\begin{aligned} |h_p^{in}(g(x)) - h_p(g(x))|^2 &= (h_p)^2(g(x)) \\ &\leq (C \cdot \sigma)^2 + (h_p)^2(g(x)) \cdot \mathbf{1}_{\mathbf{e}_{N_{sh}}^c}. \end{aligned} \quad (21)$$

As a result, we derive that:

$$\begin{aligned} \mathbb{E}[(h_p^* - h_p)^2] &\lesssim \mathbb{E}\left[\frac{\mathcal{R}(\mathcal{H})}{N_{sh} \sum_{j=1}^{N_{tr}} m_{jp}} \cdot \mathbf{1}_{\mathbf{e}_{N_{sh}}}\right] \\ &+ \sigma^2 + \mathbb{E}\left[(h_p)^2(g(x)) \cdot \mathbf{1}_{\mathbf{e}_{N_{sh}}^c}\right]. \end{aligned} \quad (22)$$

For the initial term, let $S = \sum_{i=1}^{N_{tr}} \mathbf{1}\{\|Z_k - Z_i\| < \sigma\}$. Considering Z^{un} are uniformly distributed over $[0, 1]^p$, S follows a binomial distribution $\mathcal{B}(N_{tr}, \varepsilon)$, where $\varepsilon = \mathbb{P}(\|Z - Z_k\| < \sigma)$. Utilizing the properties of the binomial distribution, we establish that:

$$\mathbb{E}\left[\frac{\mathbf{1}\{S > 0\}}{S}\right] \lesssim \frac{1}{N_{tr}\varepsilon} \lesssim \frac{1}{N_{tr}\sigma^k}. \quad (23)$$

Hence, the initial term is bounded by:

$$\mathbb{E}\left[\frac{\mathcal{R}(\mathcal{H})}{N_{sh} \sum_{j=1}^{N_{tr}} m_{jp}} \cdot \mathbf{1}_{\mathbf{e}_{N_{sh}}}\right] \lesssim \frac{\mathcal{R}(\mathcal{H})}{N_{sh} N_{tr} \sigma^k}, \quad (24)$$

The third term can be bounded in a similar fashion:

$$\begin{aligned} &\mathbb{E}\left[(h_p)^2(g(x)) \cdot \mathbf{1}_{\mathbf{e}_{N_{sh}}^c}\right] \\ &\sup(h_p)^2(g(x)) \mathbb{E}[(1 - q)^{N_{tr}}] \\ &\lesssim \sup(h_p)^2(g(x)) \frac{1}{N_{tr}q} \\ &\lesssim \frac{1}{N_{tr}\sigma^k}. \end{aligned} \quad (25)$$

By amalgamating all components, we arrive at:

$$\mathbb{E}[(h_p^* - h_p)^2] \lesssim \sigma^2 + \frac{\mathcal{R}(\mathcal{H})/N_{sh}}{N_{tr}\sigma^k}. \quad (26)$$

Given that ℓ is Lipschitz continuous with respect to its first parameter, the following inequality is obtained:

$$\begin{aligned} &\mathbb{E}_{(x,y) \sim P_t} \left[\ell(\hat{f}_\theta^{(t)}(x), y) \right] - \mathbb{E}_{(x,y) \sim P_t} \left[\ell(f_\theta^{(t)}(x), y) \right] \\ &\leq \mathbb{E} \left[|\hat{h}^{(t)} - h^{(t)}| \right] \\ &\leq \sqrt{\mathbb{E} \left[(\hat{h}^{(t)} - h^{(t)})^2 \right]} \\ &\lesssim \sigma + \sqrt{\frac{\mathcal{R}(\mathcal{H})/N_{sh}}{N_{tr}\sigma^k}}. \end{aligned} \quad (27)$$

So far, we have completed the proof of Theorem 2.

B.3 Proof of Theorem 3

Theorem 3 Consider the function class \mathcal{H} that satisfies Assumption 1 and the same conditions as Theorem 2, define the excess risk with task relation matrix \mathcal{M} by $r(\mathcal{F}_\theta^*, \mathcal{M}) = \sum_{(x,y) \in \mathcal{D}^{te}} [\ell(\mathcal{F}_\theta^*(x), y; \mathcal{M}) - \ell(\mathcal{F}_\theta(x), y; \mathcal{M})]$, we have $\inf_{\mathcal{F}_\theta^* h \in \mathcal{H}} \sup_{\mathcal{F}_\theta^* h \in \check{\mathcal{M}}} r(\mathcal{F}_\theta^*, \mathcal{M}) - \inf_{\mathcal{F}_\theta^* h \in \check{\mathcal{M}}} \sup_{\mathcal{F}_\theta^* h \in \mathcal{H}} r(\mathcal{F}_\theta^*, \check{\mathcal{M}}) < 0$.

Proof If we treat all training tasks as equally important, meaning $m_{ip} = 1$ for all τ_i and τ_p , we can express the estimator h_p as:

$$h_p = \frac{\sum_{i=1}^{N_{tr}} m_{ip} h_p}{\sum_{j=1}^{N_{tr}} m_{jp}} = \frac{1}{N_{tr}} \sum_{i=1}^{N_{tr}} h_p. \quad (28)$$

To show that this estimator performs worse than the optimal estimator h_p^* in the minimax sense which is the classifier head of the trained model \mathcal{F}_θ^* , we need to find an $h \in \mathcal{H}$ such that $\mathcal{R}_h(h^{sum}(f(x))) = \Omega(1)$ even as $N_i^{tr}, N_{tr} \rightarrow \infty$. Here, we denote h^{sum} as the average estimator of all tasks.

Consider the following setting: let $d \sim \mathcal{U}(0, 1)$ be uniformly distributed on $(0, 1)$ and let $g(x) \sim \mathcal{N}(0, 1)$ be normally distributed with mean 0 and variance 1. Define $h^d(g(x)) = d \cdot g(x)$. Under this setting, the average estimator h^{sum} becomes $h^{sum} = \frac{1}{2}g(x)$ since the expectation of d over a uniform distribution on $[0, 1]$ is $\frac{1}{2}$. To compute the risk, we calculate:

$$\mathbb{E}[(h^{sum}(g(x)) - h^d(g(x)))^2] = \mathbb{E}\left[\left(\frac{1}{2}g(x) - d \cdot g(x)\right)^2\right]. \quad (29)$$

Simplifying inside the expectation, we get:

$$\mathbb{E}\left[\left(\left(\frac{1}{2} - d\right)g(x)\right)^2\right] = \mathbb{E}\left[\left(\frac{1}{2} - d\right)^2\right] \cdot \mathbb{E}[g(x)^2]. \quad (30)$$

Since $\mathbb{E}[g(x)^2] = 1$ (the variance of $g(x)$), we need to find $\mathbb{E}\left[\left(\frac{1}{2} - d\right)^2\right]$:

$$\mathbb{E}\left[\left(\frac{1}{2} - d\right)^2\right] = \int_0^1 \left(\frac{1}{2} - d\right)^2 dd. \quad (31)$$

Evaluating this integral, we have:

$$\begin{aligned} &\mathbb{E}\left[\left(\frac{1}{2} - d\right)^2\right] \\ &= \int_0^1 \left(\frac{1}{4} - d + d^2\right) dd \\ &= \left[\frac{1}{4}d - \frac{d^2}{2} + \frac{d^3}{3}\right]_0^1 \\ &= \frac{1}{4} - \frac{1}{2} \cdot \frac{1}{2} + \frac{1}{3} = \frac{1}{12}. \end{aligned} \quad (32)$$

Therefore, we get:

$$\mathbb{E}[(h^{sum}(g(x)) - h^d(g(x)))^2] = \frac{1}{12} = \Omega(1). \quad (33)$$

Since the model $\mathcal{F}_\theta = h \circ g$ and the excess risk with task relation matrix \mathcal{M} is denoted by $r(\mathcal{F}_\theta^*, \mathcal{M}) = \sum_{(x,y) \in \mathcal{D}^{te}} [\ell(\mathcal{F}_\theta^*(x), y; \mathcal{M}) - \ell(\mathcal{F}_\theta(x), y; \mathcal{M})]$, we have:

$$\inf_{\mathcal{F}_\theta^* h \in \mathcal{H}} \sup_{\mathcal{F}_\theta^* h \in \check{\mathcal{M}}} r(\mathcal{F}_\theta^*, \mathcal{M}) - \inf_{\mathcal{F}_\theta^* h \in \check{\mathcal{M}}} \sup_{\mathcal{F}_\theta^* h \in \mathcal{H}} r(\mathcal{F}_\theta^*, \check{\mathcal{M}}) < 0. \quad (34)$$

This completes the proof.

C Datasets

In this section, we elucidate the datasets encompassed within the four experimental scenarios.

C.1 Regression

We select the Regression problem with two datasets as our inaugural experimental scenario, i.e., Sinusoid and Harmonic datasets. The datasets here consist of data points generated by a variety of sinusoidal functions, with a minimal number of data points per class or pattern. Each data point comprises an input value x and its corresponding target output value y . Typically, the input values for these data points fluctuate within a confined range, such as between 0 and 2π .

In our experiment, we enhance the complexity of the originally straightforward problem by incorporating noise. Specifically, for Sinusoid regression, we adhere to the configuration proposed by (Jiang et al. 2022; Wang et al. 2023a), where the data for each task is formulated as $A \sin(\omega \cdot x) + b + \epsilon$, with A ranging from 0.1 to 5.0, ω from 0.5 to 2.0, and b from 0 to 2π . Subsequently, we introduce Gaussian observational noise with a mean of 0 and a variance of 0.3 for each data point derived from the target task. Similarly, the Harmonic dataset (Lacoste et al. 2018) is a synthetic dataset sampled from the sum of two sine waves with different phases, amplitudes, and a frequency ratio of 2: $f(x) = a_1 \sin(\omega x + b_1) + a_2 \sin(2\omega x + b_2)$, where $y \sim \mathcal{N}(f(x), \sigma_y^2)$. Each task in the Harmonic dataset is sampled with $\omega \sim \mathcal{U}(5, 7)$, $(b_1, b_2) \sim \mathcal{U}(0, 2\pi)^2$, and $(a_1, a_2) \sim \mathcal{N}(0, 1)^2$. This process finalizes the construction of the dataset for this scenario.

C.2 Image Classification

For our second scenario, image classification, we select four benchmark datasets with two experimental settings, including standard few-shot learning (SFSL) with miniImagenet (Vinyals et al. 2016; Lin et al. 2023; Zhang et al. 2024) and Omniglot (Lake, Salakhutdinov, and Tenenbaum 2019), and cross-domain few-shot learning (CFSL) with CUB (Welinder et al. 2010) and Places (Zhou et al. 2017). We now provide an overview of the four datasets in this scenario.

- miniImagenet consists of 50,000 training images and 10,000 testing images, evenly spread across 100 categories. The first 80 of these categories are designated for training, while the final 20 are reserved for testing, with the latter never encountered during the training phase. All images are sourced from Imagenet.
- Omniglot is designed to foster the development of learning algorithms that mimic human learning processes. It encompasses 1,623 unique handwritten characters from 50 distinct alphabets, each drawn by 20 different individuals through Amazon’s Mechanical Turk. Each character image is paired with stroke data sequences $[x, y, t]$ and temporal coordinates (t) in milliseconds.
- CUB is extensively utilized for tasks involving the fine-grained differentiation of visual categories. It encompasses a collection of 11,788 photographs, categorized into 200 distinct bird species, with 5,994 images designated for training purposes and 5,794 for testing. The dataset provides comprehensive annotations for each photograph, including a single subcategory label, the precise locations of 15 parts, 312 binary attributes, and a

single bounding box. We split all the data into 100/50/50 classes for meta-training/validation/testing.

- Places is a comprehensive image collection designed for the task of scene recognition, a critical area within the field of computer vision. It boasts an extensive library of over 2.5 million images, meticulously categorized into 205 unique scene categories. Each image is meticulously curated to represent a wide array of natural and man-made environments, providing a rich tapestry of visual data for training and evaluating machine learning models. We split them into 103/51/51 classes for meta-training/validation/testing.

Note that the models in the SFSL setting are trained and tested on their evaluation datasets, while the models in the CFSL setting are trained on the miniImagenet dataset and then tested on the CUB or Places datasets.

C.3 Drug Activity Prediction

In our third scenario, concerning drug activity prediction, we align with the data partitioning delineated in (Martin et al. 2019; Jiang et al. 2022). We extract 4276 tasks from the ChEMBL database (Gaulton et al. 2012) to constitute our baseline dataset, which is preprocessed in accordance with the guidelines set forth by (Martin et al. 2019).

ChEMBL is a comprehensive database utilized extensively in chemical biology and drug research, housing a wealth of biological activity and chemical information. It contains over 1.9 million compounds, more than 2 million bioactivity assay results, and thousands of biological targets, all meticulously structured. This includes the structural data of drug compounds, bioactivity assay outcomes, and descriptions of drug targets. Following the approach in (Martin et al. 2019), we segregate the training compounds in the support set from the testing compounds in the query set, with the meta-training, meta-validation, and meta-testing task distribution being 4100, 76, and 100, respectively.

C.4 Pose Prediction

For our final scenario, we select the Pascal 3D dataset (Xiang, Mottaghi, and Savarese 2014) as our benchmark and process it accordingly. We randomly select 50 objects for meta-training and an additional 15 objects for meta-testing.

The Pascal 3D dataset is composed of outdoor images, featuring 12 classes of rigid objects chosen from the Pascal VOC 2012 dataset, each annotated with pose information such as azimuth, elevation, and distance to the camera. The dataset also includes pose-annotated images for these 12 categories from the ImageNet dataset. For the pose task, we preprocess it to include 50 categories for meta-training and 15 for meta-testing, with each category comprising 100 grayscale images, each measuring 128×128 pixels.

D Baselines

In this paper, we focus on the generalization of meta-learning and select four optimization-based meta-learning methods as the backbone for evaluating the performance of TRLearner, i.e., MAML (Finn, Abbeel, and Levine 2017), MetaSGD (Li et al. 2017), ANIL (Raghu et al. 2019a), and

Model	Omniglot		miniImagenet		miniImagenet→CUB		miniImagenet→Places	
	20-way 1-shot	20-way 5-shot	5-way 1-shot	5-way 5-shot	5-way 1-shot	5-way 5-shot	5-way 1-shot	5-way 5-shot
Meta-Trans	87.39 ± 0.51	92.13 ± 0.19	35.19 ± 1.58	54.31 ± 0.88	36.21 ± 1.36	52.78 ± 1.91	31.97 ± 0.52	\
MR-MAML	89.28 ± 0.59	95.01 ± 0.23	35.01 ± 1.60	55.06 ± 0.91	35.76 ± 1.27	50.85 ± 1.65	31.23 ± 0.48	46.41 ± 1.22
iMOL	92.89 ± 0.44	97.58 ± 0.34	36.27 ± 1.54	57.14 ± 0.87	37.14 ± 1.17	51.21 ± 1.01	32.44 ± 0.65	47.55 ± 0.94
OOD-MAML	93.01 ± 0.50	98.06 ± 0.27	37.43 ± 1.47	57.68 ± 0.85	39.62 ± 1.34	52.65 ± 0.77	35.52 ± 0.69	\
RotoGBML	92.77 ± 0.69	98.42 ± 0.31	39.32 ± 1.62	58.42 ± 0.83	41.27 ± 1.24	\	31.23 ± 0.48	\
MAML	87.15 ± 0.61	93.51 ± 0.25	33.16 ± 1.70	51.95 ± 0.97	33.62 ± 1.18	49.15 ± 1.32	29.84 ± 0.56	43.56 ± 0.88
MAML + Meta-Aug	89.77 ± 0.62	94.56 ± 0.20	34.76 ± 1.52	54.12 ± 0.94	34.58 ± 1.24	\	30.57 ± 0.63	\
MAML + MetaMix	91.97 ± 0.51	97.95 ± 0.17	38.97 ± 1.81	58.96 ± 0.95	36.29 ± 1.37	\	31.76 ± 0.49	\
MAML + Dropout-Bins	92.89 ± 0.46	98.03 ± 0.15	39.66 ± 1.74	59.32 ± 0.93	37.41 ± 1.12	\	33.69 ± 0.78	\
MAML + MetaCRL	93.00 ± 0.42	98.39 ± 0.18	41.55 ± 1.76	60.01 ± 0.95	38.16 ± 1.27	\	35.41 ± 0.53	\
MAML + TRLearner	94.23 ± 0.56	98.74 ± 0.24	42.86 ± 1.83	61.74 ± 0.96	40.54 ± 1.26	54.51 ± 0.66	36.12 ± 0.64	48.22 ± 0.95
ProtoNet	89.15 ± 0.46	94.01 ± 0.19	33.76 ± 0.95	50.28 ± 1.31	34.28 ± 1.14	48.62 ± 0.99	30.43 ± 0.57	43.40 ± 0.88
ProtoNet + Meta-Aug	90.87 ± 0.52	94.17 ± 0.25	33.95 ± 0.98	50.85 ± 1.16	35.67 ± 1.31	\	31.27 ± 0.62	\
ProtoNet + MetaMix	91.08 ± 0.51	94.32 ± 0.29	34.23 ± 1.55	51.77 ± 0.89	37.19 ± 1.24	\	31.85 ± 0.64	\
ProtoNet + Dropout-Bins	92.13 ± 0.48	94.89 ± 0.23	34.62 ± 1.54	52.13 ± 0.97	37.86 ± 1.36	\	32.59 ± 0.53	\
ProtoNet + MetaCRL	93.09 ± 0.25	95.34 ± 0.18	34.97 ± 1.60	53.09 ± 0.93	38.67 ± 1.25	\	33.82 ± 0.71	\
ProtoNet + TRLearner	94.56 ± 0.39	96.76 ± 0.24	35.45 ± 1.72	54.62 ± 0.95	39.41 ± 1.26	55.13 ± 1.32	34.54 ± 0.64	49.00 ± 0.74
ANIL	89.17 ± 0.56	95.85 ± 0.19	34.96 ± 1.71	52.59 ± 0.96	35.74 ± 1.16	49.96 ± 1.55	31.64 ± 0.57	44.90 ± 1.32
ANIL + Meta-Aug	90.46 ± 0.47	96.31 ± 0.17	35.44 ± 1.73	56.46 ± 0.95	36.32 ± 1.28	\	32.58 ± 0.64	\
ANIL + MetaMix	92.88 ± 0.51	98.36 ± 0.13	37.82 ± 1.75	59.03 ± 0.93	36.89 ± 1.34	\	33.72 ± 0.61	\
ANIL + Dropout-Bins	92.82 ± 0.49	98.42 ± 0.14	38.09 ± 1.76	59.17 ± 0.94	38.24 ± 1.17	\	33.94 ± 0.66	\
ANIL + MetaCRL	92.91 ± 0.52	98.77 ± 0.15	38.55 ± 1.81	59.68 ± 0.94	39.68 ± 1.32	\	34.47 ± 0.52	\
ANIL+ TRLearner	93.24 ± 0.48	99.28 ± 0.21	38.73 ± 1.84	60.42 ± 0.95	41.96 ± 1.24	56.22 ± 1.25	35.68 ± 0.61	47.30 ± 1.30
MetaSGD	87.81 ± 0.61	95.52 ± 0.18	33.97 ± 1.34	52.14 ± 0.92	33.65 ± 1.13	50.00 ± 0.84	29.83 ± 0.66	45.21 ± 0.79
MetaSGD + Meta-Aug	88.56 ± 0.57	96.73 ± 0.14	35.76 ± 0.91	58.65 ± 0.94	34.73 ± 1.32	\	31.49 ± 0.54	\
MetaSGD + MetaMix	93.44 ± 0.45	98.24 ± 0.16	40.28 ± 1.64	60.19 ± 0.96	35.26 ± 1.21	\	32.76 ± 0.59	\
MetaSGD + Dropout-Bins	93.93 ± 0.40	98.49 ± 0.12	40.31 ± 0.96	60.73 ± 0.92	37.49 ± 1.37	\	33.21 ± 0.67	\
MetaSGD + MetaCRL	94.12 ± 0.43	98.60 ± 0.15	41.22 ± 1.41	60.88 ± 0.91	38.61 ± 1.25	\	35.83 ± 0.63	\
MetaSGD+TRLearner	94.57 ± 0.49	99.43 ± 0.22	41.64 ± 0.94	62.43 ± 0.96	39.58 ± 1.13	57.56 ± 1.12	36.42 ± 0.54	48.20 ± 0.69
T-NET	87.66 ± 0.59	95.67 ± 0.20	33.69 ± 1.72	54.04 ± 0.99	34.82 ± 1.17	\	28.77 ± 0.48	\
T-NET + MetaMix	93.16 ± 0.48	98.09 ± 0.15	39.18 ± 1.73	59.13 ± 0.99	35.42 ± 1.28	\	30.54 ± 0.57	\
T-NET + Dropout-Bins	93.54 ± 0.49	98.27 ± 0.14	39.06 ± 1.72	59.25 ± 0.97	37.22 ± 1.37	\	31.28 ± 0.61	\
T-NET + MetaCRL	93.81 ± 0.52	98.56 ± 0.14	40.08 ± 1.74	59.40 ± 0.98	37.49 ± 1.14	\	32.37 ± 0.55	\
T-NET+TRLearner	94.33 ± 0.54	98.84 ± 0.17	40.31 ± 1.75	61.26 ± 0.97	40.64 ± 1.29	\	34.76 ± 0.62	\

Table 6: Full results (accuracy $\pm 95\%$ confidence interval) of image classification on (5-way 1-shot and 5-way 5-shot) miniImagenet and (20-way 1-shot and 20-way 5-shot) Omniglot. The best results are highlighted in **bold**. The “+” and “-” indicate the performance changes after adding MetaMix, Dropout-Bins, and MetaCRL. The “\” denotes that the result is not reported.

Model	Group 1			Group 2			Group 3			Group 4			Group 5 (ave)		
	Mean	Med.	> 0.3	Mean	Med.	> 0.3	Mean	Med.	> 0.3	Mean	Med.	> 0.3	Mean	Med.	> 0.3
MAML	0.371	0.315	52	0.321	0.254	43	0.318	0.239	44	0.348	0.281	47	0.341	0.260	45
MAML+Dropout-Bins	0.410	0.376	60	0.355	0.257	48	0.320	0.275	46	0.370	0.337	56	0.380	0.314	52
MAML+MetaCRL	0.413	0.378	61	0.360	0.261	50	0.334	0.282	51	0.375	0.341	59	0.371	0.316	56
MAML+TRLearner	0.418	0.380	62	0.366	0.263	52	0.342	0.285	52	0.379	0.339	59	0.378	0.319	56
ProtoNet	0.361	0.306	51	0.319	0.269	47	0.309	0.264	44	0.339	0.289	47	0.332	0.282	47
ProtoNet + Dropout-Bins	0.391	0.358	59	0.336	0.271	48	0.314	0.268	45	0.376	0.341	57	0.354	0.309	52
ProtoNet + MetaCRL	0.409	0.398	62	0.379	0.292	52	0.331	0.300	52	0.385	0.356	59	0.381	0.336	56
ProtoNet + TRLearner	0.436	0.402	63	0.384	0.306	54	0.357	0.313	53	0.398	0.372	61	0.393	0.348	57
ANIL	0.355	0.296	50	0.318	0.297	49	0.304	0.247	46	0.338	0.301	50	0.330	0.284	48
ANIL+MetaMix	0.347	0.292	49	0.302	0.258	45	0.301	0.282	47	0.348	0.303	51	0.327	0.284	48
ANIL+Dropout-Bins	0.394	0.321	53	0.338	0.271	48	0.312	0.284	46	0.368	0.297	50	0.350	0.271	49
ANIL+MetaCRL	0.401	0.339	57	0.341	0.277	49	0.312	0.291	48	0.371	0.305	53	0.356	0.303	51
ANIL+TRLearner	0.402	0.341	57	0.347	0.276	49	0.320	0.296	48	0.374	0.306	53	0.364	0.304	51
MetaSGD	0.389	0.305	50	0.324	0.239	46	0.298	0.235	41	0.353	0.317	52	0.341	0.274	47
MetaSGD + MetaMix	0.364	0.296	49	0.312	0.267	48	0.271	0.230	45	0.338	0.319	51	0.321	0.278	48
MetaSGD + Dropout-Bins	0.390	0.302	57	0.358	0.339	56	0.316	0.269	43	0.360	0.311	50	0.356	0.315	51
MetaSGD + MetaCRL	0.398	0.295	59	0.356	0.340	59	0.321	0.271	44	0.373	0.324	55	0.362	0.307	54
MetaSGD + TRLearner	0.403	0.314	61	0.367	0.351	60	0.345	0.284	46	0.385	0.328	56	0.374	0.319	55

Table 7: Full results on drug activity prediction. “Mean”, “Mde.”, and “> 0.3” are the mean, the median value of R^2 , and the number of analyzes for $R^2 > 0.3$ stands as a reliable indicator in pharmacology. The best results are highlighted in **bold**.

Model	10-shot	15-shot
Meta-Trans	2.671 \pm 0.248	2.560 \pm 0.196
MR-MAML	2.907 \pm 0.255	2.276 \pm 0.169
MAML	3.113 \pm 0.241	2.496 \pm 0.182
MAML + MetaMix	2.429 \pm 0.198	1.987 \pm 0.151
MAML + Dropout-Bins	2.396 \pm 0.209	1.961 \pm 0.134
MAML + MetaCRL	2.355 \pm 0.200	1.931 \pm 0.134
MAML + TRLearner	2.334 \pm 0.216	1.875 \pm 0.132
ProtoNet	3.571 \pm 0.215	2.650 \pm 0.210
ProtoNet + MetaMix	3.088 \pm 0.204	2.339 \pm 0.197
ProtoNet + Dropout-Bins	2.761 \pm 0.198	2.011 \pm 0.188
ProtoNet + MetaCRL	2.356 \pm 0.171	1.879 \pm 0.200
ProtoNet + TRLearner	2.341 \pm 0.150	1.860 \pm 0.354
ANIL	6.921 \pm 0.415	6.602 \pm 0.385
ANIL + MetaMix	6.394 \pm 0.385	6.097 \pm 0.311
ANIL + Dropout-Bins	6.289 \pm 0.416	6.064 \pm 0.397
ANIL + MetaCRL	6.287 \pm 0.401	6.055 \pm 0.339
ANIL + TRLearner	6.287 \pm 0.268	6.047 \pm 0.315
MetaSGD	2.811 \pm 0.239	2.017 \pm 0.182
MetaSGD + MetaMix	2.388 \pm 0.204	1.952 \pm 0.134
MetaSGD + Dropout-Bins	2.369 \pm 0.217	1.927 \pm 0.120
MetaSGD + MetaCRL	2.362 \pm 0.196	1.920 \pm 0.191
MetaSGD + TRLearner	2.357 \pm 0.188	1.893 \pm 0.176
T-NET	2.841 \pm 0.177	2.712 \pm 0.225
T-NET + MetaMix	2.562 \pm 0.280	2.410 \pm 0.192
T-NET + Dropout-Bins	2.487 \pm 0.212	2.402 \pm 0.178
T-NET + MetaCRL	2.481 \pm 0.274	2.400 \pm 0.171
T-NET + TRLearner	2.476 \pm 0.248	2.398 \pm 0.167

Table 8: Performance (MSE \pm 95% confidence interval) comparison on pose prediction. The best results are highlighted in **bold**.

T-Net (Lee and Choi 2018). Meanwhile, we also select multiple baselines for comparison, including regularizers which handle meta-learning generalization (Li et al. 2018b; Wang, Qiang, and Zheng 2024), i.e., Meta-Aug (Rajendran, Irpan, and Jang 2020), MetaMix (Yao et al. 2021), Dropout-Bins (Jiang et al. 2022) and MetaCRL (Wang et al. 2023a), and the SOTA methods which are newly proposed for generalization, i.e., Meta-Trans (Bengio et al. 2019), MR-MAML (Yin et al. 2020), iMOL (Wu et al. 2023), OOD-MAML (Jeong and Kim 2020), and RotoGBML (Zhang et al. 2023). Here, we briefly introduce all the methods used in our experiments.

MAML (Model-Agnostic Meta-Learning) is a widely used meta-learning algorithm that seeks to find a model initialization capable of being fine-tuned to new tasks with a few gradient steps. It focuses on learning an initialization that facilitates rapid adaptation.

MetaSGD is a meta-learning algorithm that adapts the learning rate during the meta-training process. It focuses on optimizing the learning rate, potentially improving the model’s ability to generalize across tasks.

ANIL (Almost No Inner Loop) aims to reduce the number of inner loop iterations during meta-learning. It optimizes the meta-learner by minimizing the reliance on costly inner loop optimization steps, aiming for more efficient training.

T-NET (Task-Agnostic Network) is an architecture that learns a shared representation across tasks. It aims to de-

Model	5-shot	10-shot
MAML	0.593 \pm 0.120	0.166 \pm 0.061
MAML + MetaMix	0.476 \pm 0.109	0.085 \pm 0.024
MAML + MetaCRL	0.440 \pm 0.079	0.054 \pm 0.018
MAML + MetaMix + MetaCRL	0.441 \pm 0.081	0.053 \pm 0.019
MAML + MetaMix + TRLearner	0.398 \pm 0.047	0.050 \pm 0.015
MAML + MetaCRL + TRLearner	0.395 \pm 0.050	0.047 \pm 0.019
ANIL	0.541 \pm 0.118	0.103 \pm 0.032
ANIL + MetaMix	0.514 \pm 0.106	0.083 \pm 0.022
ANIL + MetaCRL	0.468 \pm 0.094	0.081 \pm 0.019
ANIL + MetaMix + MetaCRL	0.465 \pm 0.096	0.080 \pm 0.019
ANIL + MetaMix + TRLearner	0.465 \pm 0.090	0.070 \pm 0.021
ANIL + MetaCRL + TRLearner	0.462 \pm 0.046	0.066 \pm 0.021
T-NET	0.564 \pm 0.128	0.111 \pm 0.042
T-NET + MetaMix	0.498 \pm 0.113	0.094 \pm 0.025
T-NET + MetaCRL	0.462 \pm 0.078	0.071 \pm 0.019
T-NET + MetaMix + MetaCRL	0.465 \pm 0.102	0.077 \pm 0.018
T-NET + MetaMix + TRLearner	0.440 \pm 0.065	0.061 \pm 0.012
T-NET + MetaCRL + TRLearner	0.437 \pm 0.042	0.054 \pm 0.009

Table 9: Performance (MSE) comparison on the sinusoid regression problem. The “\” denotes that the result is not reported. The best results are highlighted in **bold**.

velop a task-agnostic feature extractor that captures common patterns in different tasks, thereby improving generalization.

Meta-Aug is built by using data augmentation in the meta-learning process, with the goal of generating more diverse training samples to improve the generalization ability of the model. This includes common data augmentation techniques such as random cropping, rotation, and scaling.

MetaMix aimed at enhancing generalization in meta-learning tasks. It employs techniques to improve the model’s capability to handle variations and adapt to new tasks more effectively.

Dropout-Bins utilizes dropout techniques to improve generalization in meta-learning. These techniques enhance model robustness and help mitigate overfitting.

MetaCRL is based on causal inference and explores the task confounder problem existing in meta-learning to eliminate confusion, improving the generalization and transferability of meta-learning.

Meta-Trans combines transfer learning and meta-learning to fine-tune the pre-trained model to adapt to new tasks. The model is adjusted based on existing knowledge to improve the generalization ability on new tasks.

MR-MAML addresses the bias introduced by task overlap by designing a meta-regularization objective using information theory that prioritizes data-driven adaptation. This leads the meta-learner to decide what must be learned from the task training data and what should be inferred from the task test inputs.

iMOL is proposed for continuously adaptive out-of-distribution (CAOOD) detection, whose goal is to develop an OOD detection model that can dynamically and quickly adapt to emerging distributions and insufficient ID samples during deployment. It is worth noting that in order to adapt iMOL to the tasks of regression, classification, etc. in this paper, we rewrote the loss function of the method.

OOD-MAML is a meta-learning method for out-of-

Model	Omniglot	miniImagenet
MAML	87.15 ± 0.61	33.16 ± 1.70
MAML + MetaMix	91.97 ± 0.51	38.97 ± 1.81
MAML + MetaCRL	93.00 ± 0.42	41.55 ± 1.76
MAML + MetaMix + MetaCRL	92.88 ± 0.45	41.57 ± 1.74
MAML + MetaMix + TRLearner	94.91 ± 0.61	43.15 ± 1.17
MAML + MetaCRL + TRLearner	95.01 ± 0.71	43.84 ± 1.55
ANIL	89.17 ± 0.56	34.96 ± 1.71
ANIL + MetaMix	92.88 ± 0.51	37.82 ± 1.75
ANIL + MetaCRL	92.91 ± 0.52	38.55 ± 1.81
ANIL + MetaMix + MetaCRL	92.99 ± 0.51	38.60 ± 1.79
ANIL + MetaMix + TRLearner	93.51 ± 0.48	\
ANIL + MetaCRL + TRLearner	94.13 ± 0.62	\
MetaSGD	87.81 ± 0.61	33.97 ± 0.92
MetaSGD + MetaMix	93.44 ± 0.45	40.28 ± 0.96
MetaSGD + MetaCRL	94.12 ± 0.43	41.22 ± 0.93
MetaSGD + MetaMix + MetaCRL	94.08 ± 0.44	41.20 ± 0.95
MetaSGD + MetaMix + TRLearner	94.62 ± 0.50	\
MetaSGD + MetaCRL + TRLearner	95.00 ± 0.71	\
T-NET	87.66 ± 0.59	33.69 ± 1.72
T-NET + MetaMix	93.16 ± 0.48	39.18 ± 1.73
T-NET + MetaCRL	93.81 ± 0.52	40.08 ± 1.74
T-NET + MetaMix + MetaCRL	93.91 ± 0.52	40.15 ± 1.74
T-NET + MetaMix + TRLearner	94.81 ± 0.56	\
T-NET + MetaCRL + TRLearner	95.20 ± 0.47	\

Table 10: Performance (accuracy ± 95% confidence interval) of image classification on Omniglot and miniImagenet. The “\” denotes that the result is not reported. The best results are highlighted in **bold**.

distribution data. It improves the generalization ability of the model by learning tasks on different distributions, especially when facing new distributions.

RotoGBML homogenizes the gradients of OOD tasks, thereby capturing common knowledge from different distributions to improve generalization. RotoGBML uses reweighted vectors to dynamically balance different magnitudes to a common scale, and uses rotation matrices to rotate conflicting directions to be close to each other.

These methods and backbones are critical components of the experimental setup and are used to construct a comprehensive empirical analysis in this paper.

E Implementation and Architecture

Within the meta-learning framework, we utilize the Conv4 architecture (Finn, Abbeel, and Levine 2017; Wang and Yu 2022) as the basis for the feature extractor. After the convolution and filtering steps, we sequentially apply batch normalization, ReLU activation, and 2×2 max pooling (achieved via stride convolutions). The final output from the feature extractor’s last layer is then fed into a softmax layer with N_{tr} heads as classifiers. For one batch of training, we use different heads to participate in the training of task-specific models and introduce relation-aware consistency regularizers to participate in the update of the second layer. These network architectures undergo a pretraining phase and remain unchanged during the training process. Notably, as described in (Jiang et al. 2022; Wang et al. 2024a), we employ a different architecture for pose prediction experiments. This model consists of a fixed encoder with three convo-

lutional blocks and an adaptive decoder with four convolutional blocks. Each block includes a convolutional layer, batch normalization, and ReLU activation. For the optimization process, we use the Adam optimizer to train our model, with momentum set at 0.8 and weight decay at 0.7×10^{-5} . The initial learning rate for all experiments is 0.1, with the option for linear scaling as needed.

F Additional Results

In this section, we illustrate the additional experiments and the full results of the comparison mentioned in Section “Experiment”, including the details of motivating experiments, full results of comparison experiments, results together with task augmentation, trade-off performance comparison, OOD generalization performance comparison, and task relation visualization.

F.1 Details of Motivating Experiment

To validate our hypotheses about the errors of meta-learning paradigm, we conduct a toy experiment. We randomly select 20 sets of tasks from the miniImagenet dataset (Vinyals et al. 2016) following the method in (Wang et al. 2024b). The adaptive sampler (Wang et al. 2024b) we used here is the same as mentioned in Section “Extracting Task Relations” which aims to sample task-specific meta-data for each task. It conduct three metric, i.e., task diversity, task entropy and task difficulty, which considers four important indicators to perform task sampling, i.e., intra-class compaction, inter-class separability, feature space enrichment, and causal invariance. In this experiment, we use the three metrics to calculate the score of the 20 sets of sampled task. Among these tasks, we identify the top four tasks with the highest scores as \mathcal{D}_1 to \mathcal{D}_4 , and the bottom four tasks as \mathcal{D}_5 to \mathcal{D}_8 . Higher sampling scores indicate more complex tasks, providing the model with more information. We then apply four-fold data augmentation to \mathcal{D}_1 to \mathcal{D}_4 . Finally, we assess the MAML model’s adaptation on these eight task sets by performing a single gradient descent and recording the accuracy.

Ideally, \mathcal{D}_1 to \mathcal{D}_4 not only contain more information, but also further enhance the sample diversity through augmentation. Therefore, the model performs better after training on these four groups of tasks, and there is no overfitting. However, as shown in Figure 1, in the initial stage of the model, that is, under the constraint of limited training time, the model will be lower than the effect of training on \mathcal{D}_5 to \mathcal{D}_8 . Therefore, it will face the limitation of underfitting since it only perform one step of gradient optimization. This further verifies our point of view, i.e., MAML has the limitations of overfitting and underfitting which is caused by its own learning paradigm. Further, in order to evaluate the impact of introducing TRLearner on the model, we experimented with MAML+TRLearner under the same setting. The results are shown in Figure 6. The results show that after the introduction of TRLearner, the overfitting and underfitting phenomena of the model are greatly alleviated.

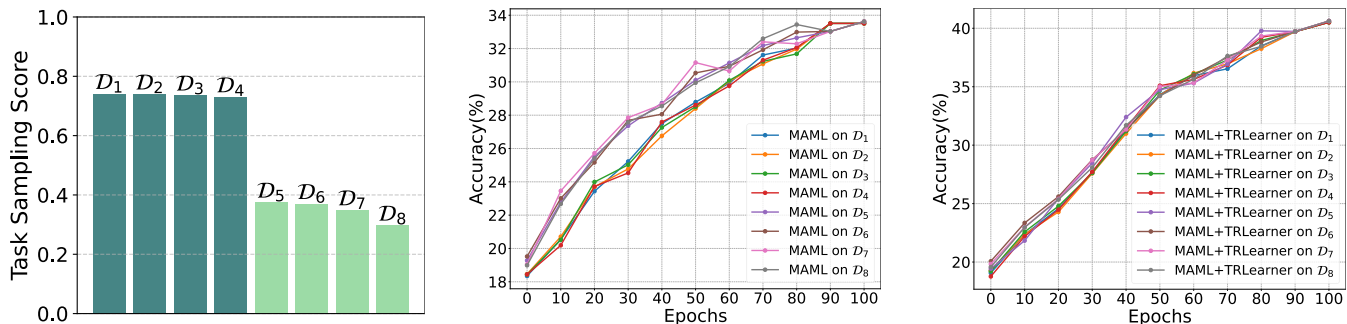


Figure 6: Performance comparison of motivating experiment after introducing TRLearner. **Left:** The score of the sampled tasks. **Middle:** Results of motivating experiment with MAML. **Right:** Results of motivating experiment with MAML+TRLearner.

F.2 Full Results of Comparison Experiments

We provide a comprehensive set of experimental results for the scenarios of image classification, drug activity prediction, and pose prediction in Tables 6, 7, and 8, respectively. The specific experimental configurations for these three scenarios are detailed in the ‘‘Experiment’’ section of the main text, with further elaboration available in the appendix. The findings confirm that, as expected, introducing TRLearner consistently delivers comparable performance across all cases.

F.3 Results Together with Other Regularizers

Although the regularization methods we choose all focus on the generalization of meta-learning, they each consider different aspects such as task augmentation and task confounder. Depending on the differences between different scenarios, the use of different solutions varies greatly. e.g., the research insights proposed in (Yao et al. 2021) show that data augmentation improves the model more significantly in the pose prediction scenario. Therefore, in order to further evaluate the potential of our method, we introduce TRLearner on the basis of introducing the regularization baselines. The results are shown in Table 9 and Table 10. We can observe that the introduction of TRLearner can achieve continuous and stable improvements. Therefore, our work focuses on the task relation that has been ignored by previous methods, while effectively improving the generalization of meta-learning.

F.4 Trade-off Performance Comparison

According to the above analysis, TRLearner improves the generalization of meta-learning in multiple scenarios. Considering that TRLearner may bring additional computational overhead due to the introduction of regularization terms, we evaluate the trade-off performance of the meta-learning model after introducing TRLearner to ensure the actual effect of TRLearner. Specifically, we use MAML as a baseline, conduct experiments on the miniImagenet dataset, and evaluate its accuracy, training time, and parameter size after introducing different methods. Figure 7 shows the trade-off performance. From the results, we can observe that after introducing TRLearner, the model achieves a significant per-

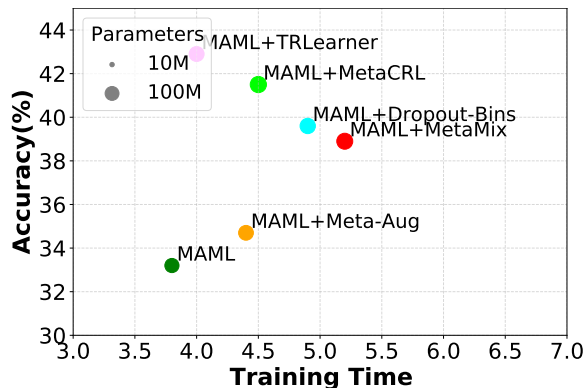


Figure 7: Trade-off performance comparison on miniImagenet. We select MAML as the meta-learning baseline.

formance improvement with acceptable calculational cost and parameter size compared to the original framework. Compared with the other baselines, it even achieves faster convergence on the basis of the effect advantage.

F.5 OOD Generalization Performance Comparison

To demonstrate the effect of TRLearner on improving generalization ability, we strengthened the distribution difference between training and testing tasks to evaluate its improvement on OOD generalization of meta-learning.

Specifically, in addition to the classification experiments in the cross-domain few-shot learning scenario, we also select a set of benchmark datasets that are most commonly used for OOD generalization verification, i.e., Meta-dataset (Triantafillou et al. 2019). This benchmark serves as a substantial resource for few-shot learning, encompassing a total of 10 datasets that span a variety of distinct domains. It is crafted to reflect a more authentic scenario by not confining few-shot tasks to a rigid set of ways and shots. The dataset encompasses 10 varied domains, with the initial 8 in-domain (ID) datasets designated for meta-training, which include ILSVRC, Omniglot, Aircraft, Birds, Textures, Quick Draw,

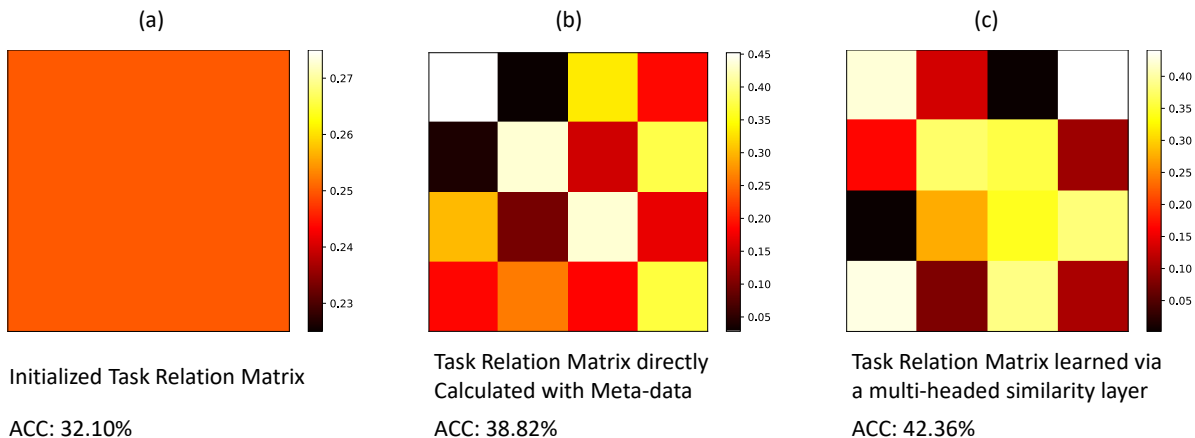


Figure 8: Task Relation Visualization. (a), (b), and (c) respectively represent the initialized task relation matrix, the task relation matrix directly calculated based on the extracted task-specific meta-data, and the task relation matrix further learned using a multi-headed similarity layer. Note that when we visualize the task relation matrix, we normalize the values in each matrix, i.e., the sum of similarity weights between the same task and other tasks is 1.

Model	Overall	ID	OOD
MAML	24.51 ± 0.13	31.37 ± 0.09	19.19 ± 0.10
MAML + MetaMix	24.94 ± 0.15	33.91 ± 0.12	20.00 ± 0.11
MAML + MetaCRL	29.65 ± 0.22	36.56 ± 0.15	24.71 ± 0.14
MAML + TRLearner	33.01 ± 0.27	41.12 ± 0.15	29.49 ± 0.12
ProtoNet	37.92 ± 0.19	42.18 ± 0.17	30.89 ± 0.11
ProtoNet + MetaMix	37.54 ± 0.21	42.56 ± 0.16	31.15 ± 0.13
ProtoNet + MetaCRL	38.91 ± 0.20	44.27 ± 0.14	33.02 ± 0.12
ProtoNet + TRLearner	40.41 ± 0.21	44.18 ± 0.16	35.15 ± 0.12

Table 11: Evaluation (accuracy ± 95% confidence interval) of OOD generalization on Meta-Dataset. The overall results are not the average of ID (in-domain) results and OOD (out-of-domain) results, but rather obtained by training on all ten datasets of Meta-Dataset.

Fungi, and VGG Flower. The final 2 datasets are earmarked for assessing out-of-domain (OOD) performance, namely Traffic Signs and MSCOCO. We assess the efficacy of meta-learning models across these 10 domains, utilizing diverse samplers across the entire suite of 10 datasets. We first sample the metadata of training and testing tasks based on the adaptive sampler (Wang et al. 2024b). Then, we record the performance changes of the meta-learning model before and after the introduction of TRLearner.

The results are shown in Table 11. The results show that after the introduction of TRLearner, meta-learning achieves a significant performance improvement, reaching 4% on average. This further illustrates the impact of task relation on OOD generalization.

E.6 Task Relation Visualization

In this subsection, we visualize the task relation extracted by TRLearner. Specifically, we visualize the initialized task relation matrix, the task relation matrix directly calculated

based on the extracted task-specific meta-data, and the task relation matrix further learned using a multi-headed similarity layer. Taking miniImagenet as an example, we set a training batch including 4 tasks and visualize the matrix and model effect after 100 epochs of training. The visualization results are shown in Figure 8. We can observe that the task relation matrix learned based on the multi-headed similarity layer is more accurate, and the meta-learning model learned based on it has the best effect. The results further demonstrate the effect of TRLearner and the importance of task relations.